

Synthesis, characterization and biological application of cyclometalated heteroleptic platinum(II) complexes

Miral V. Lunagariya | Khyati P. Thakor | Nikita J. Patel | Mohan N. Patel 

Department of Chemistry, Sardar Patel University, Vallabh Vidyanagar 388 120 Gujarat, India

Correspondence

Mohan N. Patel, Department of Chemistry, Sardar Patel University, Vallabh Vidyanagar 388 120, Gujarat, India.
Email: jeenen@gmail.com

Abstract

A series of square planar cyclometalated heteroleptic platinum(II) complexes of the type $[(C^N)Pt(O^O)]$ [where, O^O is a β -diketonato ligand of acetylacetonate (acac), C^N = cyclometalating 7-(4-fluorophenyl)-5-phenylpyrazolo[1,5-a]pyrimidine (L^1), 7-(4-chlorophenyl)-5-phenylpyrazolo[1,5-a]pyrimidine (L^2), 7-(4-bromophenyl)-5-phenylpyrazolo[1,5-a]pyrimidine (L^3), 7-(4-methoxyphenyl)-5-phenylpyrazolo[1,5-a]pyrimidine (L^4), 5-phenyl-7-(p-tolyl)pyrazolo[1,5-a]pyrimidine (L^5)] have been designed, synthesized and characterized. All compounds have been screened for biological studies like *in vitro* antibacterial, *in vitro* cytotoxicity, cellular level cytotoxicity, absorption titration, viscosity measurements, fluorescence quenching analysis, molecular docking and DNA nuclease. The intrinsic binding constants (K_b) of compounds with HS-DNA has been obtained in range of $2.892\text{--}0.242 \times 10^5 \text{ M}^{-1}$. All the compounds bound with HS DNA by partial intercalative mode of binding. MIC study has been carried out against Gram^(+ve) and Gram^(-ve) bacterial species. *In vitro* cytotoxicity against brine shrimp lethality bioassay has been also carried out. The LC_{50} values of the ligands and complexes have been found in range of 56.49–120.22 $\mu\text{g/mL}$ and 6.71–11.96 $\mu\text{g/mL}$, respectively.

KEYWORDS

Cyclometalated heteroleptic Pt(II) complexes, DNA interaction studies, *In vitro* antibacterial assay, *In vitro* cytotoxicity assay, N-donor bidentate ligands, Pyrazolo[1,5-a]pyrimidine based neutral C

1 | INTRODUCTION

Cisplatin is one of the most effective antitumor drugs widely used in cancer treatments.^[1] The anti-carcinogenic study of cisplatin has been discovered in 1960s. Cisplatin has established for clinical use in the late 1970s and platinum(II) compounds are now the important anticancer drugs on the market and used in treatment of solid tumours such as testicular, ovarian, head, neck, cervical and bladder carcinoma.^[2,3]

Although its treatment with cisplatin is restricted due to unwanted side effects like nephrotoxicity, nausea, vomiting, myelosuppression and ototoxicity.^[1] The

biological screening of platinum(II) complexes was revealed by Rosenberg and co-workers showing the ability of cisplatin to relate non-covalently with nucleoside and nucleotide.

Pyrazolo[1,5-a]pyrimidines based compounds such as ocinaplon, zaleplon and indiplon are considered as an important skeleton in a class of heterocycles and widely used in material science, natural products and pharmaceutical chemistry due to their effective bioactivities.^[4] The pyrazolo[1,5-a]pyrimidine drugs are also used in the treatment of some neurological disorders containing schizophrenia, attention deficit disorder, and Parkinson's disease.^[5]

In present work, the synthesis, characterization and their biological application of C, N –donor new class of different substituted heterocyclic pyrazolo[1,5-a]pyrimidine based bidentate ligands (L^1-L^5) and O, O –donor of acetylacetone have been used in cyclometalated heteroleptic platinum(II) complexes (I-V).

2 | EXPERIMENTAL SECTION

2.1 | Chemicals and materials

MilliQ™ (18.2 m, Millipore) was used for the preparation of deionized water. K_2PtCl_4 salts was purchased from S. D Fine-Chem Ltd. (SDFCL). Herring sperm (HS) DNA, 3-amino pyrazole, 4-methoxy benzaldehyde, 4-fluoro benzaldehyde, 4-chloro benzaldehyde, 4-bromo benzaldehyde, 4-methyl benzaldehyde and acetophenone were purchased from Sigma Aldrich Chemical Co. (India). *S. pombe* Var. Paul Linder 3360 was obtained from IMTECH, Chandigarh, India. An *Artemia* cyst was purchased from local aquarium store. Nutrient broth (NB), agarose, ethidium bromide (EtBr), tris-acetyl-EDTA (TAE), bromophenol blue was purchased from Himedia (India). The bacterial cultures were purchased from MTCC, Institute of Microbial Technology and Chandigarh, India. Thin layer chromatography (TLC) was performed using Merck aluminium sheets coated with silica gel plates (silica gel 60 F₂₅₄ 0.25 mm). Purification by flash chromatography was performed using Merck silica gel 60. and components were visualized by observation under UV light. GenElute mini Pre Kit for pUC19 DNA isolation was purchased from Sigma Aldrich (India). HPLC grade DMSO was used to dissolve the platinum(II) complexes.

2.2 | Physical measurements

Infrared spectra were recorded on a FT-IR ABB Bomen MB-3000 spectrophotometer (Canada) in the range of 4,000 to 400 cm^{-1} . 1H NMR and ^{13}C NMR spectra were recorded on Bruker Avance nuclear magnetic resonance spectrometer, either in D_2O (25 °C) or $DMSO-d_6$ (35 °C), and TMS as an internal orientation. The APT experiment yields methine (CH) and methyl (CH_3) signals negative and quaternary (C) and methylene (CH_2) signals positive. The mass spectra were obtained on a Thermo scientific mass spectrophotometer (USA) using the positive electrospray ionisation mode. Micro elemental analysis C, H, N and S of the synthesized compounds was performed with a model Euro EA elemental analyser. Melting points (°C, uncorrected) were determined in open capillaries on thermoCal10 melting point apparatus (Analab Scientific Pvt. Ltd, Vadodara, India). Antibacterial

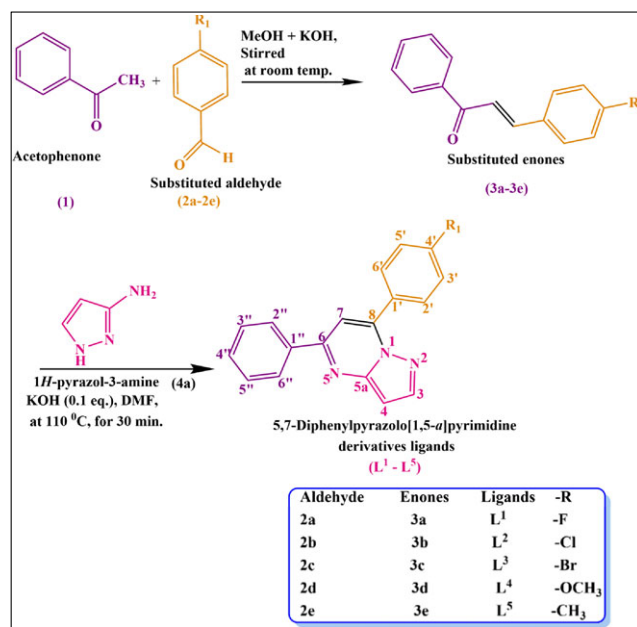
study was carried out by laminar airflow cabinet Toshiba, Delhi (India). The electronic spectra were recorded on a UV-160A UV-vis spectrophotometer, Shimadzu, Kyoto (Japan). The magnetic moments were measured by Gouy's method using mercury tetrathiocyanatocobaltate(II) as the calibrate ($\chi_{eg} = 16.44 \times 10^{-6}$ cgs units at 20 °C) citizen balance. The thermogram of complexes was recorded with a Mettler Toledo TGA Thermogravimetric analyser. Photo quantization of the gel after electrophoresis was done using AlphaDigiDoc™ Version V.4.0.0 PC-Image software, California (USA). Conductance measurement was carried out using conductivity meter model number E-660A. Fluorescence spectroscopy was carried out by FluoroMax-4, spectrofluorometer, HORIBA (Scientific).

2.3 | Synthesis of α,β unsaturated carbonyl compounds (3a – 3e)

The α,β unsaturated carbonyl compounds (3a-3f) have been synthesized using literature procedure.^[2] The proposed reaction mechanism for the synthesis of chalcone is shown in Scheme 1.

2.4 | Synthesis of pyrazolo[1,5-a]pyrimidine derivatives ligands (L^1-L^5)

Synthesis of the pyrazolo[1,5-a]pyrimidines based ligands (L^1-L^5) have been carried out using Lipson and co-workers reported method^[3]. To a solution of the α,β unsaturated carbonyl compounds (3a-3f) (2.95 mmol) in



SCHEME 1 Reaction scheme of the synthesized different substituted pyrazolo[1,5-a] pyrimidine based ligands ($L^1 - L^5$)

10 mL of DMF, 1*H*-pyrazol-3-amine (4a) (0.245 g, 2.95 mmol) and KOH (0.25 g, 0.1 mmol) solution were added. The reaction mixture was refluxed for 30 min. Upon completion of reaction as indicated by TLC plates, the excess of solvent was removed under reduced pressure and the reaction mixture was cooled on an ice bath. The reaction mixture was extracted with ethylacetate (50 mL × 3) and washed thoroughly with water (30 mL × 3). The brine solution of sodium chloride was added to it and dried over sodium sulphate. The resulting mixture was concentrated under vacuum. The residue was purified by column chromatography on silica gel system (ethylacetate: hexane, 4:1) to obtain the pyrazolo[1,5-*a*]pyrimidine based ligands as a product. The proposed reaction mechanism for the synthesis of ligands (3a-3f) is shown in Scheme 1. The ¹H NMR and ¹³C NMR spectra of ligands are shown in supplementary material 1 and 2, respectively.

2.5 | Characterization of 7-(4-fluorophenyl)-5-phenylpyrazolo[1,5-*a*]pyrimidine (L¹)

This ligand (L¹) has prepared through the addition of enone (3a) (816 mg, 2.958 mmol) and 1*H*-pyrazole-3-amine (4a) (245 mg, 2.958 mmol). Colour: lemon yellow powder, Yield: 87%, mol. Wt.: 289.31 g/mol, m.p.: 180 °C, Chemical formula C₁₈H₁₂FN₃. ¹H NMR (400 MHz, DMSO-*d*₆) δ/ppm: 8.297 (3H, t, ³J₁ = 6.8 Hz, ³J₂ = 6.8 Hz, H_{3'',4'',5''}), 8.257 (1H, d, J₁ = 7.6 Hz, H₃), 8.153 (2H, d, J₁ = 8.0 Hz, H_{3',5'}), 7.742 (1H, s, H₇), 7.534 (2H, dd, ³J₁ = 8.0 Hz, ⁴J₂ = 2.0 Hz, H_{2'',6''}), 7.410 (2H, d, J = 8.0 Hz, H_{2',6'}), 6.830 (1H, d, J = 8.0 Hz, H₄). ¹³C NMR (100 MHz, DMSO-*d*₆) δ/ppm: 162.72 (C₄, C_{quat.}), 155.71 (C₆, C_{quat.}), 149.70 (C_{5a}, C_{quat.}), 145.53 (C₈, C_{quat.}), 145.46 (C₃, -CH), 137.22 (C_{1''}, C_{quat.}), 132.88 (C_{2',6'}, -CH), 132.79 (C_{3'',5''}, -CH), 130.96 (C_{4''}, -CH), 129.34 (C_{2'',6''}, -CH), 127.81 (C_{1'}, C_{quat.}), 116.01 (C_{5',3'}, -CH), 105.36 (C₇, -CH), 97.28 (C₄, -CH). [Total signal observed = 14: signal of C = 6 (p-F-phenyl ring-C = 2, pyrazolo[1,5-*a*]pyrimidine-C = 3, phenyl ring-C = 1), signal of CH = 8 (pyrazolo[1,5-*a*]pyrimidine-CH = 3, p-F-phenyl ring-CH = 2, phenyl ring-CH = 3)]. FT-IR: (KBr) (cm⁻¹): 2923 ν_{(C-H)ar}, 1550 ν_(C=N), 1504 ν_{(C-H)banding}, 1218 ν_(C-N), 1604 ν_{(C=C)conjugated alkenes}, 763 ν_{(Ar-H)2 adjacent hydrogen}. Mass (m/z): 290 [M]⁺, 195, 119.

2.6 | Characterization of 7-(4-chlorophenyl)-5-phenylpyrazolo[1,5-*a*]pyrimidine (L²)

This ligand (L²) has prepared through the addition of enone (3b) (868 mg, 2.958 mmol) and 1*H*-pyrazole-3-

amine (4a) (245 mg, 2.958 mmol). Colour: lemon yellow powder, Yield: 90%, mol. wt.: 305.77 g/mol, m.p.: 170 °C, Anal. Calc. (%) For C₁₈H₁₂ClN₃: C, 70.71; H, 3.96; N, 13.74 Found (%): C, 70.39; H, 3.83; N, 13.67. ¹H NMR (400 MHz, DMSO-*d*₆) δ/ppm: 8.307 (3H, t, ³J₁ = 6.8 Hz, ³J₂ = 6.8 Hz, H_{3'',4'',5''}), 8.259 (1H, d, J = 8.0 Hz, H₃), 8.157 (2H, d, J = 8.4 Hz, H_{3',5'}), 7.746 (1H, s, H₇), 7.544 (2H, dd, ⁴J₁ = 8.0 Hz, ³J₂ = 2.4 Hz, H_{2'',6''}), 7.426 (2H, d, J = 8.0 Hz, H_{2',6'}), 6.837 (1H, d, J = 8.0 Hz, H₄). ¹³C NMR (100 MHz, DMSO-*d*₆) δ/ppm: 155.64 (C₆, C_{quat.}), 149.76 (C_{5a}, C_{quat.}), 146.48 (C₈, C_{quat.}), 145.44 (C₃, -CH), 141.46 (C_{1''}, C_{quat.}), 137.31 (C_{4'}, C_{quat.}), 130.86 (C_{1'}, C_{quat.}), 130.07 (C_{5',3'}, -CH), 129.37 (C_{3'',5''}, -CH), 129.30 (C_{2',6'}, -CH), 128.47 (C_{4''}, -CH), 127.76 (C_{2'',6''}, -CH), 104.91 (C₇, -CH), 97.10 (C₄, -CH). [Total signal observed = 14: signal of C = 6 (p-Cl-phenyl ring-C = 2, pyrazolo[1,5-*a*]pyrimidine-C = 3, phenyl ring-C = 1), signal of CH = 8 (pyrazolo[1,5-*a*]pyrimidine-CH = 3, p-F-phenyl ring-CH = 2, phenyl ring-CH = 3)]. FT-IR: (KBr) (cm⁻¹): 2931 ν_{(C-H)ar}, 1550 ν_(C=N), 1504 ν_{(C-H)banding}, 1218 ν_(C-N), 1605 ν_{(C=C)conjugated alkenes}, 764 ν_{(Ar-H)2 adjacent hydrogen}. Mass (m/z): 306 [M]⁺, 307 [M + 2], 195, 119.

2.7 | Characterization of 7-(4-bromophenyl)-5-phenylpyrazolo[1,5-*a*]pyrimidine (L³)

This ligand (L³) has prepared through the addition of enone (3c) (999 mg, 2.958 mmol) and 1*H*-pyrazole-3-amine (4a) (245 mg, 2.958 mmol). Colour: pale yellow powder, Yield: 94%, mol. wt.: 350.22 g/mol, m.p.: 173 °C, Anal. Calc. (%) For C₁₈H₁₂BrN₃: C, 61.73; H, 3.45; N, 12.00 Found (%): C, 61.49; H, 3.32; N, 12.07. ¹H NMR (400 MHz, DMSO-*d*₆) δ/ppm: 8.299 (3H, t, ³J₁ = 6.8 Hz, ³J₂ = 6.8 Hz, H_{3'',4'',5''}), 8.235 (1H, d, J = 8.0 Hz, H₃), 8.136 (2H, d, J = 8.0 Hz, H_{3',5'}), 7.740 (1H, s, H₇), 7.539 (2H, dd, ⁴J₁ = 8.0 Hz, ³J₂ = 3.6 Hz, H_{2'',6''}), 7.428 (2H, d, J = 8.0 Hz, H_{2',6'}), 6.833 (1H, d, J = 8.0 Hz, H₄). ¹³C NMR (100 MHz, DMSO-*d*₆) δ/ppm: 155.66 (C₆, C_{quat.}), 149.77 (C_{5a}, C_{quat.}), 146.52 (C₈, C_{quat.}), 145.47 (C₃, -CH), 141.49 (C_{1''}, C_{quat.}), 137.32 (C_{3',5'}, -CH), 130.89 (C_{3'',5''}, -CH), 130.10 (C_{4''}, -CH), 129.40 (C_{2',6'}, -CH), 129.33 (C_{2'',6''}, -CH), 128.49 (C_{1'}, C_{quat.}), 127.78 (C_{4'}, C_{quat.}), 104.94 (C₇, -CH), 97.12 (C₄, -CH). [Total signal observed = 14: signal of C = 6 (p-Br-phenyl ring-C = 2, pyrazolo[1,5-*a*]pyrimidine-C = 3, phenyl ring-C = 1), signal of CH = 8 (pyrazolo[1,5-*a*]pyrimidine-CH = 3, p-F-phenyl ring-CH = 2, phenyl ring-CH = 3)]. FT-IR: (KBr) (cm⁻¹): 2931 ν_{(C-H)ar}, 1551 ν_(C=N), 1505 ν_{(C-H)banding}, 1226 ν_(C-N), 1604 ν_{(C=C)conjugated alkenes}, 771 ν_{(Ar-H)2 adjacent hydrogen}. Mass (m/z): 351 [M]⁺, 195, 119.

2.8 | Characterization of 7-(4-methoxyphenyl)-5-phenylpyrazolo[1,5-a]pyrimidine (L⁴)

This ligand (L⁴) has prepared through the addition of enone (3d) (854 mg, 2.958 mmol) and 1*H*-pyrazole-3-amine (4a) (245 mg, 2.958 mmol). Colour: pale yellow powder, Yield: 93%, mol. wt.: 301.35 g/mol, m.p.: 174 °C, Anal. Calc. (%) For C₁₉H₁₅N₃O: C, 75.73; H, 5.02; N, 13.94; Found (%): C, 75.49; H, 5.56; N, 13.47. ¹H NMR (400 MHz, DMSO-d₆) δ/ppm: 8.310 (3H, t, ³J₁ = 6.0 Hz, ³J₂ = 6.0 Hz, H_{3'',4'',5''}), 8.266 (1H, d, J = 6.4 Hz, H₃), 8.168 (2H, d, J = 8.0 Hz, H_{3',5'}), 7.766 (1H, s, H₇), 7.495 (2H, dd, ⁴J₁ = 8.0 Hz, ³J₂ = 5.6 Hz, H_{2'',6''}), 7.430 (2H, d, J = 8.0 Hz, H_{2',6'}), 6.837 (1H, d, J = 8.0 Hz, H₄), 2.440 (3H, s, -OCH₃). ¹³C NMR (100 MHz, DMSO-d₆) δ/ppm: 155.72 (C_{4'}, C_{quat.}), 149.68 (C₆, C_{quat.}), 145.57 (C₃, -CH), 145.26 (C₈, C_{quat.}), 137.17 (C_{5a}, C_{quat.}), 136.20 (C_{1''}, C_{quat.}), 132.07 (C_{3',5'}, -CH), 131.00 (C_{3'',5''}, -CH), 130.12 (C_{1'}, C_{quat.}), 129.36 (C_{4''}, -CH), 128.93 (C_{2',6'}, -CH), 127.81 (C_{2'',6''}, -CH), 105.50 (C₇, -CH), 97.36 (C₄, -CH), 55.50 (-O-CH₃). [Total signal observed = 15: signal of C = 6 (p-Br-phenyl ring-C = 2, pyrazolo[1,5-a]pyrimidine-C = 3, phenyl ring-C = 1), signal of CH and CH₃ = 9 (pyrazolo[1,5-a]pyrimidine-CH = 3, p-F-phenyl ring-CH = 2, phenyl ring-CH = 3, -OCH₃ = 1)]. FT-IR: (KBr) (cm⁻¹): 2931 ν_{(C-H)ar}, 1550 ν_(C=N), 1488 ν_{(C-H)banding}, 1218 ν_(C-N), 1604 ν_{(C=C)conjugated alkenes}, 763 ν_{(Ar-H)2 adjacent hydrogen}. Mass (m/z): 302 [M]⁺, 195, 119.

2.9 | Characterization of 5-phenyl-7-(p-tolyl)pyrazolo[1,5-a]pyrimidine (L⁵)

This ligand (L⁵) has prepared through the addition of enone (3e) (807 mg, 2.958 mmol) and 1*H*-pyrazole-3-amine (4a) (245 mg, 2.958 mmol). Colour: pale yellow powder, Yield: 90%, mol. wt.: 285.35 g/mol, m.p.: 176 °C, Anal. Calc. (%) For C₁₉H₁₅N₃: C, 79.98; H, 5.30; N, 14.73; Found (%): C, 79.79; H, 5.16; N, 14.44. ¹H NMR (400 MHz, DMSO-d₆) δ/ppm: 8.306 (3H, t, ³J₁ = 6.0 Hz, ³J₂ = 6.0 Hz, H_{3'',4'',5''}), 8.263 (1H, d, J = 6.4 Hz, H₃), 8.164 (2H, d, J = 8.0 Hz, H_{3',5'}), 7.762 (1H, s, H₇), 7.492 (2H, dd, ⁴J₁ = 8.0 Hz, ³J₂ = 6.4 Hz, H_{2'',6''}), 7.430 (2H, d, J = 8.0 Hz, H_{2',6'}), 6.839 (1H, d, J = 8.0 Hz, H₄), 1.640 (3H, s, -CH₃). ¹³C NMR (100 MHz, DMSO-d₆) δ/ppm: 155.36 (C₆, C_{quat.}), 149.73 (C_{5a}, C_{quat.}), 146.92 (C₈, C_{quat.}), 145.47 (C₃, -CH), 141.49 (C_{1''}, C_{quat.}), 137.39 (C_{1'}, C_{quat.}), 130.89 (C_{3',5'}, -CH), 130.10 (C_{3'',5''}, -CH), 129.80 (C_{4''}, -CH), 129.33 (C_{2',6'}, -CH), 128.48 (C_{4'}, C_{quat.}), 127.78 (C_{2'',6''}, -CH), 104.94 (C₇, -CH), 97.12 (C₄, -CH), 21.56 (-CH₃). [Total signal observed = 15: signal of C = 6 (p-Br-phenyl ring-C = 2, pyrazolo[1,5-a]pyrimidine-C = 3, phenyl ring-

C = 1), signal of CH and CH₃ = 9 (pyrazolo[1,5-a]pyrimidine-CH = 3, p-F-phenyl ring-CH = 2, phenyl ring-CH = 3, -CH₃ = 1)]. FT-IR: (KBr) (cm⁻¹): 2923 ν_{(C-H)ar}, 1542 ν_(C=N), 1488 ν_{(C-H)banding}, 1234 ν_(C-N), 1605 ν_{(C=C)conjugated alkenes}, 763 ν_{(Ar-H)2 adjacent hydrogen}. Mass (m/z): 286 [M]⁺, 195, 119.

2.10 | Preparation of heteroleptic cycloplatinated complexes (I-V)

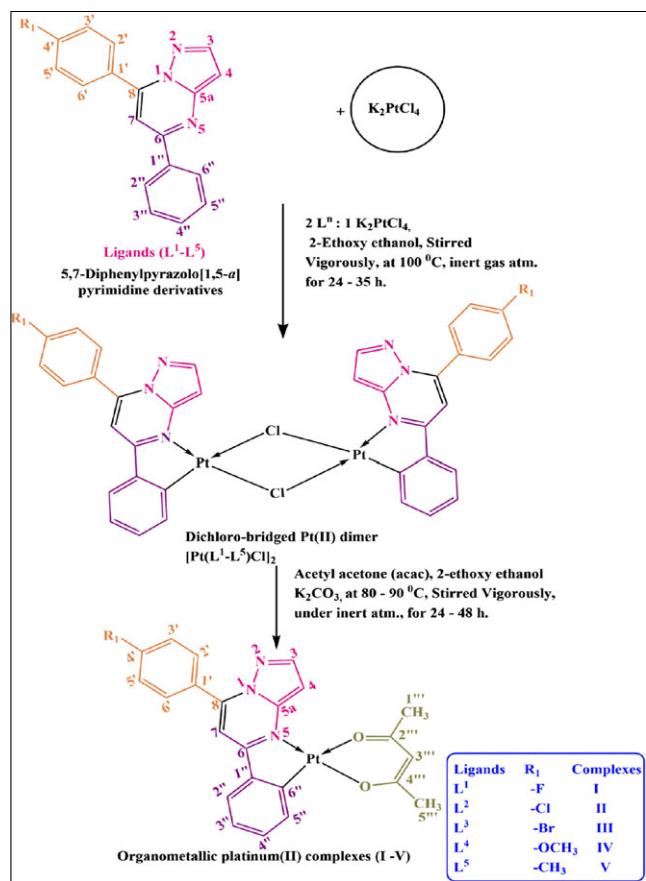
2.10.1 | General procedure for synthesis of organometallic platinum(II) complexes (I-V)

Synthesis of the platinum(II) μ-dichloro-bridged dimers have been derived following a modified method of Lewis.^[6,7] To a solution of 5,7-diphenylpyrazolo[1,5-a]pyrimidine derivatives ligand (L¹-L⁵) (58.6 mg, 0.4 mmol) and K₂PtCl₄ (83 mg, 0.2 mmol) in ethoxyethanol, stirred vigorously under nitrogen (N₂) atm. And refluxed at 100 °C for 24–35 h. The reaction mixture was allowed to cool at room temperature. The obtained precipitate (chloro-bridged Pt(II) dimer) was washed with water (20 mL) and dried at 50 °C under vacuum. The crude product was used for next step without further purification and characterization.

The crude product (chloro-bridged Pt(II) dimer) was treated with 3 molar equivalent acetyl acetone in the presence of 10 equiv. of K₂CO₃ in 2-ethoxyethanol solvent at 80–90 °C under nitrogen (N₂) atmosphere for 24–48 h. The mixture was poured into water for extraction through separating funnel using solvent dichloromethane (CH₂Cl₂). The organic extracts were washed with water and dried over anhydrous sodium sulphate. After the solvent was completely evaporated, than the obtained residue was purified by column chromatography on silica gel with dichloromethane/petroleum ether (1:1) system as the eluent to obtain pure product. The proposed reaction mechanism for the synthesis of cyclometalated heteroleptic platinum(II) complexes (I-V) are represented in Scheme 2. The ¹H NMR and ¹³C NMR spectra of platinum(II) complexes are shown in supplementary material 1 and 2, respectively.

2.10.2 | Characterization of μ-dichloro bridge platinum(II) complex (I) (dimer)

Dimer of platinum(II) complex (I) has been prepared according to the above general procedure. Characterization of this dimer by spectroscopic method like ¹H NMR and ¹³C NMR spectra are represented in supplementary material 1 and 2, respectively. Yield: 25%, mol. wt.: 1051.71 g/mol, chemical formula: C₃₇H₂₂Cl₂F₂N₆Pt₂, ¹H NMR (400 MHz, DMSO-d₆) δ/ppm: 8.713 (2H, d,



SCHEME 2 Synthesis of the cyclometalated heteroleptic platinum(II) complexes (I-V) via μ -dichloro bridge platinum(II) complex (dimer) as an intermediate

$J = 8.0$ Hz, $H_{3,3}$), 8.536 (2H, d, $J = 8.0$ Hz, $H_{4,4}$), 8.407 (4H, d, $J = 7.6$ Hz, $H_{3',5',3',5'}$), 8.178 (2H, s, $H_{7,7}$), 7.857 (4H, d, $J = 7.6$ Hz, $H_{2',6',2',6'}$), 7.708 (4H, dd, ${}^3J_1 = 8.0$ Hz, ${}^4J_2 = 5.6$ Hz, $H_{2'',5'',2'',5''}$), 7.634 (2H, t, ${}^3J_1 = 8.0$ Hz, ${}^3J_2 = 8.0$ Hz, $H_{3'',3''}$), 7.448 (2H, t, ${}^3J_1 = 8.0$ Hz, ${}^3J_2 = 8.0$ Hz, $H_{4'',4''}$). ${}^{13}\text{C}$ NMR (100 MHz, DMSO- d_6) δ /ppm: 162.79 (C_4 , C_{quat}), 155.91 (C_6 , C_{quat}), 149.70 (C_{5a} , C_{quat}), 145.53 (C_8 , C_{quat}), 145.46 (C_3 , -CH), 137.22 ($C_{1''}$, C_{quat}), 132.88 ($C_{2',6'}$, -CH), 132.79 ($C_{5''}$, -CH), 130.96 ($C_{4''}$, -CH), 129.94 ($C_{2''}$, -CH), 128.80 ($C_{1'}$, C_{quat}), 128.01 ($C_{3''}$, -CH), 127.81 ($C_{6''}$, C_{quat}), 116.21 ($C_{5',3'}$, -CH), 105.36 (C_7 , -CH), 97.22 (C_4 , -CH). [Total signal observed = 16: signal of C = 7 (p-F-phenyl ring-C = 2, pyrazolo[1,5-a]pyrimidine-C = 3, phenyl ring-C = 2), signal of CH = 9 (pyrazolo[1,5-a]pyrimidine-CH = 3, p-F-phenyl ring-CH = 2, phenyl ring-CH = 4)].

2.10.3 | Structure characterization of cycloplatinated complex [(L¹)Pt(acac)] (I)

It has prepared according to the synthetic procedure of complex (I) but the ratio among [Pt(L¹)Cl]₂ dimer and acetyl acetone, which is 1:3 mole to the described in

procedure. Colour: brown powder, Yield: 40%, mol. wt.: 582.50 g/mol, m.p.: >300 °C, Chemical formula: $\text{C}_{23}\text{H}_{18}\text{FN}_3\text{O}_2\text{Pt}$. UV-Vis: λ (nm) (ϵ , $\text{M}^{-1}\text{cm}^{-1}$): 299 (12,230), 360 (3,900). Conductance: $22\ \Omega^{-1}\text{cm}^2\text{mol}^{-1}$. ${}^1\text{H}$ NMR (400 MHz, DMSO- d_6) δ /ppm: 8.295 (2H, t, ${}^3J_1 = 6.8$ Hz, ${}^3J_2 = 6.8$ Hz, $H_{3'',4''}$), 8.256 (1H, d, $J = 8.0$ Hz, H_3), 8.151 (2H, d, $J = 8.0$ Hz, $H_{3',5'}$), 7.752 (1H, s, H_7), 7.533 (2H, dd, ${}^4J_1 = 8.0$ Hz, ${}^3J_2 = 2.0$ Hz, $H_{2'',5''}$), 7.420 (2H, d, $J = 8.0$ Hz, $H_{2',6'}$), 6.822 (1H, d, $J = 8.0$ Hz, H_4), 6.020 (1H, s, $H_{3''}$), 1.997 (3H, s, $H_{5''}$), 0.880 (3H, s, $H_{1''}$). ${}^{13}\text{C}$ NMR (100 MHz, DMSO- d_6) δ /ppm: 191.00 ($C_{2''}$, C = O), 181.89 ($C_{4''}$, C-O-Pt), 162.89 (C_4 , C_{quat}), 155.98 (C_6 , C_{quat}), 149.80 (C_{5a} , C_{quat}), 145.57 (C_3 , -CH), 145.46 (C_8 , C_{quat}), 137.72 ($C_{1''}$, C_{quat}), 132.88 ($C_{2',6'}$, -CH), 132.79 ($C_{3''}$, -CH), 130.96 ($C_{4''}$, -CH), 129.74 ($C_{5''}$, -CH), 128.80 ($C_{1'}$, C_{quat}), 128.01 ($C_{2''}$, -CH), 127.81 ($C_{6''}$, C_{quat}), 121.21 (C_7 , -CH), 116.23 ($C_{2',6'}$, -CH), 97.32 (C_4 , -CH), 81.33 ($C_{3''}$, -CH), 24.43 ($C_{5''}$, -CH₃), 16.00 ($C_{1''}$, -CH₃). [Total signal observed = 21: signal of C = 9 (p-F-phenyl ring-C = 2, pyrazolo[1,5-a]pyrimidine-C = 3, phenyl ring-C = 2, acetyl acetone (C = O) = 2), signal of CH = 12 (pyrazolo[1,5-a] pyrimidine-CH = 3, p-F-phenyl ring-CH = 2, phenyl ring-CH = 4, acetyl acetone-CH = 1, acetylacetone-CH₃ = 2)]. FT-IR: (KBr) (cm^{-1}): 3062 $\nu_{(\text{C}-\text{H})_{\text{ar}}}$, 1552 $\nu_{(\text{C}=\text{N})}$, 1496 $\nu_{(\text{C}-\text{H})}$ banding, 1789 $\nu_{(\text{C}=\text{O})}$, 1226 $\nu_{(\text{C}-\text{N})}$, 1606 $\nu_{(\text{C}=\text{C})}$ conjugated alkenes, 432 $\nu_{(\text{O}-\text{Pt})}$, 779 $\nu_{(\text{Ar}-\text{H})_2}$ adjacent hydrogen, 501 $\nu_{(\text{N}-\text{Pt})}$, 416 $\nu_{(\text{C}-\text{Pt})}$.

2.10.4 | Structure characterization of cycloplatinated complex [(L²)Pt(acac)] (II)

It has prepared according to the synthetic procedure of complex (II) but ratio among the [Pt(L²)Cl]₂ dimer and acetyl acetone, which is 1:3 mole to the described in procedure. Colour: brown powder, Yield: 35%, mol. wt.: 598.95 g/mol, m.p.: >300 °C, Anal. Calc. (%) For $\text{C}_{23}\text{H}_{18}\text{ClN}_3\text{O}_2\text{Pt}$: C, 46.12; H, 3.03; N, 7.02; Pt, 32.57; Found (%): C, 46.79; H, 3.16; N, 7.44; Pt, 32.53. Conductance: $22\ \Omega^{-1}\text{cm}^2\text{mol}^{-1}$. UV-vis: λ (nm) (ϵ , $\text{M}^{-1}\text{cm}^{-1}$): 295 (22,770), 357 (6,610). ${}^1\text{H}$ NMR (400 MHz, DMSO- d_6) δ /ppm: 8.299 (2H, t, ${}^3J_1 = 8.0$ Hz, ${}^3J_2 = 8.0$ Hz, $H_{3'',4''}$), 8.253 (1H, d, $J = 8.0$ Hz, H_3), 8.150 (2H, d, $J = 8.0$ Hz, $H_{3',5'}$), 7.750 (1H, s, H_7), 7.540 (2H, dd, ${}^4J_1 = 8.0$ Hz, ${}^3J_2 = 6.0$ Hz, $H_{2'',5''}$), 7.424 (2H, d, $J = 8.0$ Hz, $H_{2',6'}$), 6.826 (1H, d, $J = 8.0$ Hz, H_4), 6.022 (1H, s, $H_{3''}$), 1.998 (3H, s, $H_{5''}$), 0.890 (3H, s, $H_{2''}$). ${}^{13}\text{C}$ NMR (100 MHz, DMSO- d_6) δ /ppm: 190.00 ($C_{2''}$, C = O), 181.89 ($C_{4''}$, C-O-Pt), 155.94 (C_6 , C_{quat}), 149.76 (C_{5a} , C_{quat}), 146.48 (C_8 , C_{quat}), 145.44 (C_3 , -CH), 141.46 ($C_{1''}$, C_{quat}), 137.31 ($C_{4'}$, C_{quat}), 130.86 ($C_{3',5'}$, -CH), 130.07 ($C_{5''}$, -CH), 129.37 ($C_{3''}$, -CH), 129.30 ($C_{4''}$, -CH), 128.87 ($C_{1'}$, C_{quat}), 128.67 ($C_{2''}$, -CH), 128.47 ($C_{2',6'}$,

–CH), 127.16 (C₆^{''}, C_{quat.}), 121.19 (C₇, –CH), 97.90 (C₄, –CH), 81.33 (C₃^{'''}, –CH), 24.43 (C₅^{'''}, –CH₃), 16.00 (C₁^{'''}, –CH₃). [Total signal observed = 21: signal of C = 9 (p-Cl-phenyl ring-C = 2, pyrazolo[1,5-a]pyrimidine-C = 3, phenyl ring-C = 2, acetyl acetone (C = O) = 2), signal of CH and CH₃ = 12 (pyrazolo[1,5-a] pyrimidine-CH = 3, p-Cl-phenyl ring-CH = 2, phenyl ring-CH = 4, acetyl acetone-CH = 1, acetylacetone-CH₃ = 2)]. FT-IR: (KBr) (cm⁻¹): 3060 ν_{(C-H)ar}, 1551 ν_(C=N), 1488 ν_{(C-H)banding}, 1728 ν_(C=O), 1280 ν_(C-N), 1605 ν_{(C=C)conjugated alkenes}, 433 ν_(O-Pt), 764 ν_{(Ar-H)2 adjacent hydrogen}, 509 ν_(N-Pt), 417 ν_(C-Pt). LC-MS (m/z): 599.80 [M]⁺, 601.85 [M + 2].

2.10.5 | Structure characterization of cycloplatinated complex [(L³)Pt(acac)] (III)

It has prepared according to the synthetic procedure of complex (III) but the ratio among [Pt(L³)Cl]₂ dimer and acetyl acetone, which is 1:3 mole to the described in procedure. Colour: brown powder, Yield: 38%, mol. wt.: 643.40 g/mol, m.p.: >300 °C, Anal. Calc. (%) For C₂₃H₁₈BrN₃O₂Pt: C, 42.94; H, 2.82; N, 6.53; Pt, 30.32; Found (%): C, 42.49; H, 2.56; N, 6.34; Pt, 30.13. Conductance: 22 Ω⁻¹cm²mol⁻¹. UV-Vis: λ (nm) (ε, M⁻¹ cm⁻¹): 292 (12,570), 353 (2,660). ¹H NMR (400 MHz, DMSO-d₆) δ/ppm: 8.309 (2H, t, ³J₁ = 7.6 Hz, ³J₂ = 7.6 Hz, H₃^{''',4''}), 8.258 (1H, d, J = 8.0 Hz, H₃), 8.159 (2H, d, J = 8.0 Hz, H_{3',5'}), 7.742 (1H, s, H₇), 7.533 (2H, dd, ⁴J₁ = 8.0 Hz, ³J₂ = 2.0 Hz, H₂^{''',6''}), 7.417 (2H, d, J = 8.0 Hz, H_{2',6'}), 6.822 (1H, d, J = 8.0 Hz, H₄), 6.021 (1H, s, H₃^{'''}), 1.990 (3H, s, H₅^{'''}), 0.891 (3H, s, H₂^{'''}). ¹³C NMR (100 MHz, DMSO-d₆) δ/ppm: 190.00 (C₂^{''}, C = O), 181.89 (C₄^{''}, C-O-Pt), 155.98 (C₆, C_{quat.}), 149.76 (C_{5a}, C_{quat.}), 146.48 (C₈, C_{quat.}), 145.44 (C₃, –CH), 141.48 (C₁^{''}, C_{quat.}), 137.31 (C_{4'}, C_{quat.}), 130.82 (C_{3',5'}, –CH), 130.07 (C₅^{''}, –CH), 129.37 (C₃^{''}, –CH), 129.30 (C₄^{''}, –CH), 128.87 (C_{1'}, C_{quat.}), 128.62 (C₂^{''}, –CH), 128.47 (C_{2',6'}, –CH), 127.12 (C₆^{''}, C_{quat.}), 121.89 (C₇, –CH), 97.92 (C₄, –CH), 81.33 (C₃^{'''}, –CH), 24.43 (C₅^{'''}, –CH₃), 16.00 (C₁^{'''}, –CH₃). [Total signal observed = 21: signal of C = 9 (p-Br-phenyl ring-C = 2, pyrazolo[1,5-a]pyrimidine-C = 3, phenyl ring-C = 2, acetyl acetone (C = O) = 2), signal of CH and CH₃ = 12 (pyrazolo[1,5-a]pyrimidine-CH = 3, p-Br-phenyl ring-CH = 2, phenyl ring-CH = 4, acetyl acetone-CH = 1, acetylacetone-CH₃ = 2)]. FT-IR: (KBr) (cm⁻¹): 3039 ν_{(C-H)ar}, 1550 ν_(C=N), 1496 ν_{(C-H)banding}, 1774 ν_(C=O), 1265 ν_(C-N), 1605 ν_{(C=C)conjugated alkenes}, 493 ν_(O-Pt), 763 ν_{(Ar-H)2 adjacent hydrogen}, 563 ν_(N-Pt), 430 ν_(C-Pt).

2.10.6 | Structure characterization of cycloplatinated complex [(L⁴)Pt(acac)] (IV)

It has prepared according to the synthetic procedure of complex (IV) but the ratio among [Pt(L⁴)Cl]₂ dimer and

acetyl acetone, which is 1:3 mole to the described in procedure. Colour: brown powder, Yield: 35%, mol. wt.: 594.53 g/mol, m.p.: >300 °C, Anal. Calc. (%) For C₂₄H₂₁N₃O₃Pt: C, 48.49; H, 3.56; N, 7.07; Pt, 32.81; Found (%): C, 48.39; H, 3.76; N, 7.44; Pt, 32.73. Conductance: 22 Ω⁻¹cm²mol⁻¹. UV-vis: λ (nm) (ε, M⁻¹ cm⁻¹): 292 (38,830), 362 (7,390). ¹H NMR (400 MHz, DMSO-d₆) δ/ppm: 8.302 (2H, t, ³J₁ = 4.8 Hz, ³J₂ = 4.8 Hz, H₃^{''',4''}), 8.251 (1H, d, J = 8.0 Hz, H₃), 8.154 (2H, d, J = 8.0 Hz, H_{3',5'}), 7.745 (1H, s, H₇), 7.535 (2H, dd, ⁴J₁ = 8.0 Hz, ⁴J₂ = 2.0 Hz, H₂^{''',5''}), 7.427 (2H, d, J = 8.0 Hz, H_{2',6'}), 6.829 (1H, d, J = 8.0 Hz, H₄), 6.017 (1H, s, H₃^{'''}), 2.890 (3H, s, –OCH₃), 1.990 (3H, s, H₅^{'''}), 0.891 (3H, s, H₁^{'''}). ¹³C NMR (100 MHz, DMSO-d₆) δ/ppm: 190.00 (C₂^{''}, C = O), 181.89 (C₄^{''}, C-O-Pt), 155.58 (C₆, C_{quat.}), 149.56 (C_{5a}, C_{quat.}), 146.48 (C₈, C_{quat.}), 145.44 (C₃, –CH), 141.48 (C₁^{''}, C_{quat.}), 137.31 (C_{4'}, C_{quat.}), 130.82 (C_{3',5'}, –CH), 130.07 (C₅^{''}, –CH), 129.57 (C₃^{''}, –CH), 129.20 (C₄^{''}, –CH), 128.87 (C_{1'}, C_{quat.}), 128.62 (C₂^{''}, –CH), 128.47 (C_{2',6'}, –CH), 127.15 (C₆^{''}, C_{quat.}), 121.59 (C₇, –CH), 97.52 (C₄, –CH), 81.33 (C₃^{'''}, –CH), 55.98 (–OCH₃), 24.43 (C₅^{'''}, –CH₃), 16.00 (C₁^{'''}, –CH₃). [Total signal observed = 22: signal of C = 9 (p-OCH₃-phenyl ring-C = 2, pyrazolo[1,5-a] pyrimidine-C = 3, phenyl ring-C = 2, acetyl acetone (C = O) = 2), signal of CH and CH₃ = 13 (pyrazolo[1,5-a]pyrimidine-CH = 3, p-Br-phenyl ring-CH = 2, phenyl ring-CH = 4, acetyl acetone-CH = 1, acetylacetone-CH₃ = 2, –OCH₃ = 1)]. FT-IR (KBr): (cm⁻¹): 3031 ν_{(C-H)ar}, 1551 ν_(C=N), 1512 ν_{(C-H)banding}, 1773 ν_(C=O), 1266 ν_(C-N), 1604 ν_{(C=C)conjugated alkenes}, 439 ν_(O-Pt), 764 ν_{(Ar-H)2 adjacent hydrogen}, 501 ν_(N-Pt), 424 ν_(C-Pt).

2.10.7 | Structure characterization of cycloplatinated complex [(L⁵)Pt(acac)] (V)

It has prepared according to the synthetic procedure of complex (IV) but the ratio among [Pt(L⁵)Cl]₂ dimer and acetyl acetone, which is 1:3 mole to the described in procedure. Colour: brown powder, Yield: 35%, mol. wt.: 578.54 g/mol, m.p.: >300 °C, Anal. Calc. (%) For C₂₄H₂₁N₃O₂Pt: C, 49.83; H, 3.66; N, 7.26; Pt, 33.72; Found (%): C, 49.67, H, 3.56 N, 7.44; Pt, 32.73. Conductance: 22 Ω⁻¹cm²mol⁻¹. UV-Vis: λ (nm) (ε, M⁻¹ cm⁻¹): 296 (19,920), 351 (5,550). ¹H NMR (400 MHz, DMSO-d₆) δ/ppm: 8.309 (2H, t, ³J₁ = 8.0 Hz, ³J₂ = 8.0 Hz, H₃^{''',4''}), 8.252 (1H, d, J = 8.0 Hz, H₃), 8.158 (2H, d, J = 8.0 Hz, H_{3',5'}), 7.755 (1H, s, H₇), 7.534 (2H, dd, ⁴J₁ = 8.0 Hz, ³J₂ = 2.4 Hz, H₂^{''',5''}), 7.428 (2H, d, J = 8.0 Hz, H_{2',6'}), 6.824 (1H, d, J = 8.0 Hz, H₄), 6.017 (1H, s, H₃^{'''}), 2.291 (3H, s, –CH₃), 1.912 (3H, s, H₅^{'''}), 0.892 (3H, s, H₁^{'''}). ¹³C NMR (100 MHz, DMSO-d₆) δ/ppm: 190.00 (C₂^{''}, C = O), 181.89 (C₄^{''}, C-O-Pt), 155.73 (C₆, C_{quat.}), 149.66 (C_{5a},

C_{quat}), 146.38 (C_8 , C_{quat}), 145.64 (C_3 , $-\text{CH}$), 141.48 ($C_{1''}$, C_{quat}), 137.36 (C_4 , C_{quat}), 130.82 ($C_{3',5'}$, $-\text{CH}$), 130.37 ($C_{5''}$, $-\text{CH}$), 129.67 ($C_{3''}$, $-\text{CH}$), 129.20 ($C_{4''}$, $-\text{CH}$), 128.87 ($C_{1'}$, C_{quat}), 128.62 ($C_{2''}$, $-\text{CH}$), 128.47 ($C_{2',6'}$, $-\text{CH}$), 127.12 ($C_{6''}$, C_{quat}), 121.87 (C_7 , $-\text{CH}$), 97.92 (C_4 , $-\text{CH}$), 81.33 ($C_{3'''}$, $-\text{CH}$), 24.66 ($-\text{CH}_3$), 24.43 ($C_{5'''}$, $-\text{CH}_3$), 16.00 ($C_{1'''}$, $-\text{CH}_3$). [Total signal observed = 22: signal of C = 9 (p- CH_3 -phenyl ring-C = 2, pyrazolo[1,5-a] pyrimidine-C = 3, phenyl ring-C = 2, acetyl acetone (C = O) = 2), signal of CH and CH_3 = 13 (pyrazolo[1,5-a] pyrimidine-CH = 3, p- CH_3 -phenyl ring-CH = 2, phenyl ring-CH = 4, acetyl acetone-CH = 1, acetylacetone- CH_3 = 2, $-\text{CH}_3$ = 1)]. FT-IR (KBr): (cm^{-1}): 3062 $\nu_{(\text{C-H})}$ ar, 1550 $\nu_{(\text{C=N})}$, 1488 $\nu_{(\text{C-H})}$ banding, 1789 $\nu_{(\text{C=O})}$, 1272 $\nu_{(\text{C-N})}$, 1604 $\nu_{(\text{C=C})}$ conjugated alkenes, 455 $\nu_{(\text{O-Pt})}$, 763 $\nu_{(\text{Ar-H})}$ 2 adjacent hydrogen, 563 $\nu_{(\text{N-Pt})}$, 430 $\nu_{(\text{C-Pt})}$.

2.11 | Biological screening of compounds

2.11.1 | *In vitro* antibacterial activity

The MIC informs about the degree of resistance of certain bacterial species towards the test compounds. MIC value was performed by serially two fold dilution of the test compound added to three Gram^(-ve) microorganisms namely *Escherichia coli* (MTCC 433), *Pseudomonas aeruginosa* (MTCC P-09), *Serratia marcescens* (MTCC 7103) and two Gram^(+ve) bacteria namely *Bacillus subtilis* (MTCC 7193), *Staphylococcus aureus* (MTCC 3160). The lowest compound concentration inhibiting visible bacterial growth is reported as MIC.^[8,9]

2.11.2 | *In vitro* brine shrimp lethality bioassay

The cytotoxicity assay was performed on brine shrimp nauplii by Meyer method.^[10] The lethal concentrations of compounds resulting in 50% mortality (LC_{50}) of the brine shrimp from the 24 h and the dose-response data were transformed into a straight line by means of a trend line fit linear regression analysis; the LC_{50} was determined from the best-fit line, a graph of mortality vs. concentration of nauplii.^[11] The LC_{50} value is obtained the antilogarithm of $\log [\text{complex}]$ vs. 50% mortality (LC_{50}). All data has been collected from three independent experiments and the LC_{50} determined using OriginPro 8 software.

2.11.3 | Cellular level cytotoxicity against *S. Pombe* cells

Cellular level bioassay was carried out using *S. pombe* cells, which were grown in liquid yeast extract media in 150 mL Erlenmeyer flask containing 30 mL of yeast

extract media. The flask was incubated at 30 °C on a shaker at 160 rpm till the exponential growth of *S. pombe* obtained (24 to 30 h). Then the cell culture was treated with the different concentrations (20, 40, 60, 80, 100 μM) of synthesized complexes, free ligands and also with DMSO as a control and further allowed to grow for 20–24 h. Next day, by centrifugation at 12,000 rpm 10 min; treated cells were collected and dissolved in 500 mL of PBS (Phosphate Buffered Saline). The 80 mL of yeast culture dissolved in PBS and 20 mL of 0.4% trypan blue prepared in PBS were mixed and cells were observed in a compound microscope (40 X). The trypan blue dye could enter the dead cell only so they appeared blue, whereas live cells resisted the entry of dye. The number of dead cells and number of live cells was counted in one field. Cell counting was repeated in two more of the microscopic fields and average percentage of cells died due to synthesized compounds were calculated.^[12]

3 | DNA INTERACTION STUDIES

3.1 | Electronic absorption titration spectroscopy

All the experiments involving the interaction of the Pt(II) complexes (**1a-1f**) with HS DNA were used for nucleotide binding study. The stock solution was prepared by dissolving HS-DNA in a phosphate buffer (pH 7.2) containing 5% DMSO at 4 °C for complete dissolution and used within 4 days. Ratio of UV absorbance kept at 260 and 280 nm was about 1.89:1 for HS DNA in the buffer, suggesting the HS DNA sufficiently free from protein.^[13] The nucleotide binding experiments were completed at room temperature. All experiments were carried out by keeping the concentration of platinum complexes constant (400 μM) while concentrations of HS DNA were determined spectrophotometrically by assuming $\epsilon_{260} = 12558 \text{ M}^{-1} \text{ cm}^{-1}$.^[14-17]

3.2 | Viscosity measurements

Viscosity experiment was made using an Ubbelohde viscometer, engrossed in a water bath at 25.0 ± 0.5 °C. The viscosity of a 200 μM solution of HS-DNA was determined in the presence of the complexes using different $[\text{complex}]/[\text{DNA}]$ ratios in the range of 0.00 to 2.00. The flow time was measured in triplicate with a digital stopwatch and then averaged. The relative viscosity ratio (η_r) was plotted against the r -bound (where η_r and η_r^0 were the relative viscosity for DNA in the presence or absence of complexes, respectively). The hydrodynamic length of DNA generally increases upon partial intercalation while it does not lengthen

upon groove binding.^[18] Viscosity measurements can sensitively detect the lengthening of a DNA helix induced by the binding of intercalators and thus provide evidence of intercalation for small DNA-binding molecules.^[19] The data are represented as the plot of the relative viscosity, i.e. $(\eta/\eta_0)^{1/3}$ vs. $[\text{complex}]/[\text{DNA}]$.

3.3 | Fluorescence quenching analysis

Emission intensity measurements of ethidium bromide (EB = 3,8-diamino-5-ethyl-6-phenylphenanthridinium bromide) with free HS-DNA in the absence and presence of Pt(II) complexes were performed in phosphate buffer. The HS-DNA solution was up to the value of $r = 3.33$ ($[\text{DNA}]/[\text{Complex}]$) of pre-treated EB-DNA mixture ($[\text{EB}] = 33.3 \mu\text{M}$, $[\text{DNA}] = 10 \mu\text{M}$) at ambient temperature and incubate for 10 min before measurement. The emission intensity was recorded in the range of 500–800 nm. The emission intensities at 610 nm (λ_{max}) were obtained through excitation at 510 nm and slit wavelength 1.45 nm in the FluoroMax-4, HORIBA (Scientific) spectrofluorometer. The changes in fluorescence intensities of ethidium bromide and ethidium bromide bound to DNA were measured with respect to different concentration of the complex. The ethidium bromide has less-emission intensity in phosphate buffer solution 7.2 pH due to fluorescence quenching of free ethidium bromide by the solvent molecules. In the presence of DNA, EB exhibits higher intensity due to its partial intercalative binding mode to DNA. Fluorescence quenching of an EB-DNA can arise owing to inner-filter effect. The mechanism of quenching is found from the emission intensity of EB. In our study, inner filter effect was corrected with the following equation in this literature.^[20,21]

To examine the fluorescence quenching mechanism, the Stern–Volmer quenching constant (K_{sv}) was determined by equation 1.^[22,23]

$$I^0/I = K_{\text{sv}}[Q] + 1 \quad (1)$$

where, I_0 and I are the emission intensity of EB-DNA in the absence and presence of quencher (complex), K_{sv} is the linear Stern-Volmer quenching constant obtained from the plot of I_0/I vs. $[Q]$ and $[Q]$ is concentration of quencher. To determine the strength of the interaction of complexes with DNA, the value of the associative binding constant (K_a) was calculated using the Scatchard equation 2:^[24,25]

$$\log I_0 - I/I = \log K_a + n \log [Q] \quad (2)$$

where, I_0 and I are the fluorescence intensities of the EB-DNA in the absence and presence of different concentrations of complexes, respectively and n is the number of

binding. The acting forces between drugs and biomacromolecules include hydrogen bonds, van der Waals forces, electrostatic attraction and hydrophobic interaction, etc. In order to estimate the interaction force of all compounds, the standard free energy changes (ΔG) for the binding process have been calculated using the Van't Hoff equation 3:^[26]

$$\Delta G^0 = -RT \ln K_a \quad (3)$$

where, T is the temperature (25 °C, 298 K here), K_a is associative binding constant and R is gas constant $8.314 \text{ Jmol}^{-1} \text{ K}^{-1}$. The negative sign for ΔG^0 means that the binding process is spontaneous.

3.4 | Molecular modeling study

Docking study was made for Pt(II) complexes with biomolecule (DNA), to identify the binding mode of action and the vital functional groups interacting with the DNA, using Hex 8.0 software. Pt^{II} complexes were taken from their enhanced structure as a molecule and converted to .pdb (Protein Data Bank) format using CHIMERA 1.5.1 software. The change of transcription or replication of DNA may leading to gene mutation, thus causing a series of diseases, in this way it plays an irreplaceable role in life. DNA is also the target of many antibacterial drugs, antiviral, cancer and playing an important role in the treatment of diseases. HS-DNA used in the experimental work was too large for current computational resources to dock, therefore, the structure of the DNA of sequence $d(\text{ACCGACGTCGGT})_2$ (1BNA) is used for interaction study (PDB id: 1BNA, a familiar sequence used in oligodeoxynucleotide study) obtained from the Protein Data Bank (<http://www.rcsb.org/pdb>).^[27] All calculations were done using on an Intel CORE i5, 2.5 GHz based machine running MS Windows 8, 64 bit as the operating system. The by default parameters were used for the docking calculation with correlation type shape only, FFT mode at 3D level, grid dimension of 6 with receptor range 180 and ligand range 180 with twist range 360 and distance range 40. The best conformation was selected with the lowest binding energy (kJ/mol).^[28]

3.5 | Photochemical analysis of DNA nuclease activity

Gel electrophoresis study was performed using pUC19 DNA with synthesized compounds. The samples were incubated for 0.5 h at 37°C. The samples were analysed by 1% agarose gel electrophoresis [Tris–acetate–ethylene-diaminetetraacetic acid, (TAE) buffer, pH 8.0] for 3 h at 100 mV. The gel was stained with (0.5 mg mL^{-1}) ethidium

bromide. The gels were viewed in an Alpha Innotech Corporation Gel doc system and photographed using a CCD camera. The cleavage efficiency of the compounds, the degree of DNA cleavage activity was measured by determining the ability of the complex to SC-DNA to OC-DNA equation describe in literature.^[29]

4 | RESULTS AND DISCUSSION

4.1 | ¹H NMR spectra

The ¹H NMR spectra of the pyrazolo[1,5-a]pyrimidine based ligands (L¹-L⁵) and cyclometalated platinum(II) complexes (I-V) have been obtained in solvent DMSO d₆ as illustration in supplementary material 1 and the resultant physicochemical data of synthesized compounds are summarized in experimental section. In ¹H NMR spectra of synthesized ligands (L¹-F, L²-Cl, L³-Br, L⁴-OCH₃, L⁵-CH₃) the number of aromatic hydrogen atoms are 12-H (pyrazolo[1,5-a]pyrimidine derivative). While in complexes (I-V) number of aromatic and aliphatic hydrogen atoms are 11-H (pyrazolo[1,5-a]pyrimidine derivative ligand) and 7-H (acetyl acetone), respectively it indicates that carbon C_{6''} attached to central metal ion. The peak of synthesized ligands (L¹-L⁵, H_{2'',6''}) are found in the range of 7.492 to 7.534 δ ppm. These hydrogen (H_{2'',6''}) exhibit doublet of doublet (dd). It is not observed in the complexes, it indicates that platinum ion coordinated to C_{6''} carbon atom of ligands via covalent bond. Hence, one aromatic hydrogen atom less in complexes than ligands. In pyrazolo[1,5-a]pyrimidine derivatives ligands (L¹-L⁵), all the aromatic proton are observed in the range of ~δ 8.29 to 6.50 ppm and all aromatic proton of the cyclometalated platinum(II) complexes are appeared in the range of ~δ 8.309 to 6.8 ppm. Methoxy group of ligand (L⁴) and complex (IV) are appeared at about ~δ 2.44 and ~δ 2.89 ppm, respectively. Methyl (-CH₃) group of ligand (L⁵) and complex (V) are observed at about ~δ 1.640 and ~δ 2.291 ppm, respectively. All the cyclometalated platinum(II) complexes contain acetylacetone bidentate ligands. Therefore methyl group protons are obtained in range of ~δ 0.892-1.912 ppm.

4.2 | ¹³C NMR spectra

The ¹³C NMR spectra of the synthesized pyrazolo[1,5-a]pyrimidine based aromatic ligands, cyclometalated heteroleptic platinum(II) complexes and μ-dichloro bridge complex (I) are shown in supplementary material 2 and data of these compounds are represented in experimental section. The peak of ligand (L⁴) containing methoxy group and ligand (L⁵) containing methyl group

are appeared at 55.50 ppm and 21.56 ppm, respectively. These peaks are shifted to downfield in complex (IV) and complex (V) are observed at 55.98 ppm and 24.66 ppm, respectively. The cyclometalated heteroleptic platinum(II) complexes (I-V) containing acetylacetone bidentate ligands having >C = O peak observed in range of 181.89-190.00 ppm. The peak of ligand (Lⁿ, C_{6''}, -CH) are observed in the range of 127.76-129.33 ppm. It indicate that the peak observed in down part of base line in attached proton test (APT) spectra. In complexes (Pt-C_{6''}, C_{quat.}), the C_{6''} quaternary carbon atom peak is shifted to upfield in the range of 127.16-127.81 ppm, and this peak is obtained in the upper part of the base line in APT. These observation suggests that the complexes exhibit upfield shift as compared to free ligands.

4.3 | FT-IR spectroscopy

FT-IR spectral data of synthesized pyrazolo[1,5-a]pyrimidine based ligands (L¹-L⁵) and cyclometalated heteroleptic platinum(II) complexes (I-V) are presented in experimental section. The peaks of ligands containing azomethine ν(C = N) group is observed in the range of 1542-1550 cm⁻¹ and it is shifted to higher frequencies (1550-1522 cm⁻¹) in the complexation, showing the coordination of the heterocyclic nitrogen atoms (azomethine group) to platinum metal ion^[30,31] The bands νC = C_{ar} of the compounds are observed in the of range 1604-1606 cm⁻¹. The νC-H_{ar} stretching band of the free ligands are observed in the range of 2926-2930 cm⁻¹ and it is shifted to higher frequency in the range of 3050-3060 cm⁻¹ of complexes. The spectra of all the platinum(II) complexes show bands in the range of 501-563 cm⁻¹, 432-493 cm⁻¹ and 416-430 cm⁻¹, due to (Pt-N), (Pt-O) and (Pt-C), respectively. In platinum(II) complexes (I-V), the peak of acetylacetone group containing (>C = O) is observed in the range of 1728-1774 cm⁻¹.

4.4 | Mass spectroscopy

The mass spectra and fragmentation pattern of synthesized pyrazolo[1,5-a]pyrimidine based ligands (L¹-L⁵) are shown in supplementary material 3 and data of all the ligands are illustrate in experimental section. The LC-MS spectrum and possible mass fragmentation pattern of complex (II) are shown in Figure 1. The mass spectrum of a synthesized platinum(II) complex (II) shows a molecular ion peak at 599.80 m/z and 601.85 m/z due to [M]⁺ and [M + 2], respectively, it indicate that the one chlorine atom present in the complexes. The peaks at 499.84 m/z and 501 m/z is due to pyrazolo[1,5-a]pyrimidine ligands attached to platinum

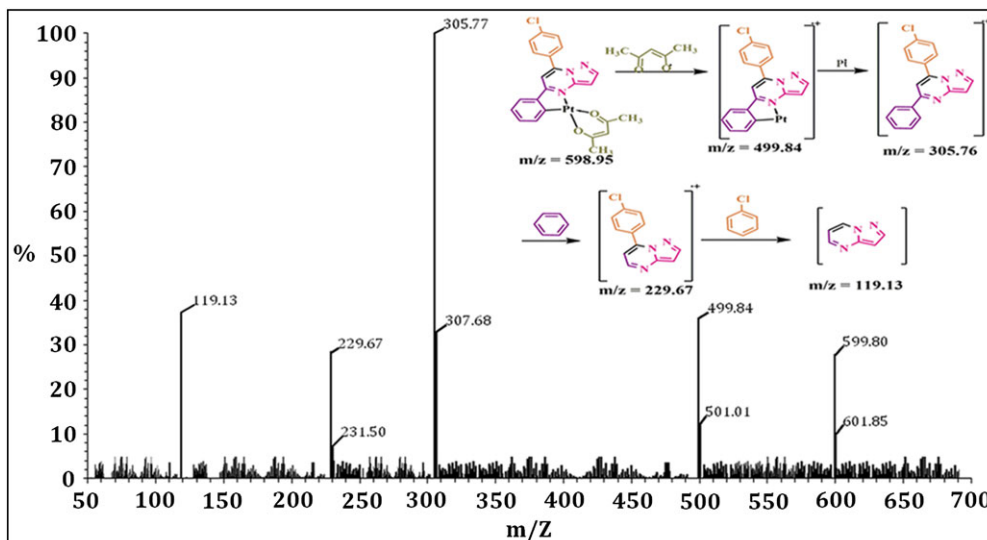


FIGURE 1 LC-MS spectrum and mass fragmentation pattern of the synthesized cyclometalated heteroleptic platinum(II) complex (II)

metal ion with loss of acetylacetonate moiety. The peaks at 305.77 m/z and 307.68 m/z corresponds to pyrazolo[1,5-a]pyrimidine based ligands. The peaks at 229.67 m/z and 231.50 m/z are obtained with loss of phenyl ring in this ligand. The peak at 119.13 m/z is observed of pyrazolo[1,5-a]pyrimidine.

4.5 | Electronic spectra, magnetic behaviour and conductance measurements

The geometry of the cyclometalated heteroleptic platinum(II) complexes has been confirmed using electronic spectral analysis. The cyclometalated platinum(II) complexes (I-V) exhibit two intense bands, in the range of 292–299 nm and 307–360 nm due to charge transfer (CT) and d-d transitions, respectively.^[1,32]

Electronic spectra of all the complexes (I-V) are represented in Figure 2. The magnetic moments of Pt(II) complexes are zero B.M. and are consistent with low-spin $t_{2g}^6 e_g^2 (d^8)$ configuration square planer geometry having dsp^2 hybridisation. All the complexes are diamagnetic in nature.^[33] The molar conductivity (Λ_m) of platinum(II) complexes are observed in the range of 18–25 $\Omega^{-1} \text{cm}^2 \text{mol}^{-1}$, which suggests the non-electrolytic nature of the complexes.

4.6 | Thermogravimetric analysis (TGA)

Thermogravimetric curve for cyclometalated heteroleptic platinum(II) complex (II) is obtained at a heating rate of 10 °C per minute in the range of 0–800 °C under dinitrogen atmosphere (See Supplementary material 4). No mass loss is observed up to 200 °C indicating the

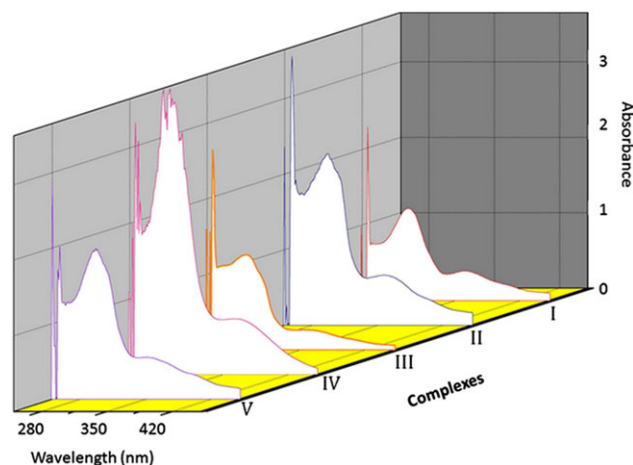


FIGURE 2 Electronic spectra of the synthesized cyclometalated heteroleptic platinum(II) complexes (I-V).

absence of co-ordinated and lattice water molecule or any volatile component. The platinum(II) complexes decomposed in two steps. First mass loss (17.01%) occurring in the temperature range of 205–270 °C corresponds to loss of acetylacetonate ligand. Second mass loss (52.49%) in the range of 280–410 °C corresponds to the loss of pyrazolo[1,5-a]pyrimidine based ligand and leaving behind metallic platinum as residue.^[33]

4.7 | Biological screening of synthesized compounds

4.7.1 | *In vitro* antibacterial activity

The study of antimicrobial potency is carried out in terms of minimum inhibitory concentration (MIC) defined as

the lowest concentration which inhibits the growth of microorganism, referred by lack of turbidity in the tube. If specific concentration for a test compounds no turbidity is observed then a whole experimental procedure is repeated with the next dilution i.e. half the inhibitory concentration (IC_{50}) of test compound that has been previously added. This procedure is repeated till the faint turbidity by the inoculums itself is observed and this concentration is termed as MIC (in μM). The result of this study are represented in the Figure 3 and data of the compounds are represented in supplementary material 5. The IC_{50} values of the complexes and ligands are observed in range of 25–95 μM and 190–270 μM , respectively. The platinum(II) complexes (I–V) exhibit higher antimicrobial activity than metal salt and free pyrazolo[1,5-a]pyrimidine based ligands (L^1 – L^5).^[34] The *in vitro* antimicrobial bioassay of the metal complexes can be described on the basis of Tweedy's chelation theory.^[35] Chelation decreases the polarity of metal ion due to partial sharing of its positive charge with donor groups and possible π -electron delocalization over the whole chelate ring. As a result lipophilic character of the central metal atom increases, approving its permeation through the lipid layer of the cell membrane and quickly attack the metal binding sites on enzymes of microorganism which inhibit the further growth of the organism.^[36]

4.7.2 | *In vitro* cytotoxicity against Artemia cyst lethality bioassay

All the synthesized compounds pyrazolo[1,5-a]pyrimidine based ligands (L^1 – L^5) and cyclometalated platinum(II) complexes (I–V) have been tested for *in vitro* brine shrimp lethality bioassay using Meyer et al. process.^[37] The percentage mortality of brine shrimp nauplii has been determined from the number of dead nauplii. The LC_{50}

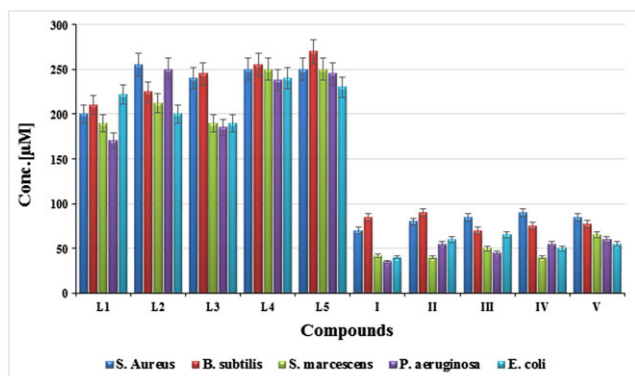


FIGURE 3 Effect of different concentrations (μM) of free ligands and platinum(II) complexes on two gram^(+ve) and three gram^(-ve) microorganisms. Error bars represent the standard deviation of three independent $\pm 5\%$

value is calculated from the plot of log of concentration of samples against percentage of mortality of nauplii and represented in Figure 4. It is concluded that the platinum(II) complexes show excellent toxicity as compared to corresponding ligands. The mortality rate of nauplii is found to increase with increasing concentration of compounds. The LC_{50} values of synthesized ligands and complexes are observed in the range of 56.49–120.22 $\mu\text{g mL}^{-1}$ and 6.714–11.96 $\mu\text{g mL}^{-1}$, respectively. The LC_{50} values of cisplatin and transplatin are 3.133 and 14.45 $\mu\text{g mL}^{-1}$. The potency of the synthesized compounds are represented in order of $L^5 < L^4 < L^3 < L^2 < L^1 < \text{transplatin} < \text{V} < \text{IV} < \text{III} < \text{II} < \text{I} < \text{cisplatin}$. *In vitro* cytotoxicity study is a basic one and additional studies are necessary to investigate its actual mechanism of cytotoxicity and its probable effects on cancer cell line.

4.7.3 | Cellular level *in vitro* cytotoxicity against *S. Pombe* cells

Cellular level *in vitro* cytotoxicity of the synthesized ligands and complexes have been tested by *S. pombe* cells. From the conclusion, cell death caused by toxicity of the synthesized compounds could be easily monitored by trypan blue dye as a staining. The potency has found to vary with the different type of functional group present and differ concentrations of the synthesized ligands and platinum(II) complexes. Complexes I, II and III (–F, –Cl and –Br) are found to be excellent toxicity as compared to other complexes (IV and V), All the platinum(II) complexes (I–V) are more toxic in nature as compared to pyrazolo[1,5-a]pyrimidine based ligands

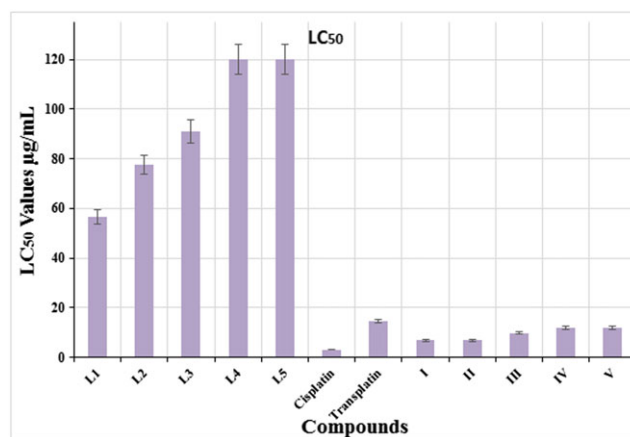


FIGURE 4 Effect of the substituted pyrazolo[1,5-a]pyrimidine based ligands (L^1 – L^5), cisplatin, transplatin and cyclometalated heteroleptic platinum(II) complexes (I–V) on the brine shrimp lethality bioassay shown with standard deviation for three times repeat experiments

(L¹-L⁵). The *in vitro* cytotoxicity potency of the platinum(II) complexes is comparable to standard drug such as cisplatin and transplatin. After 17–20 h of the treatment, many of the *S. pombe* cells are destroyed due to toxic nature of the complexes. The order of the synthesized compounds are found to be cisplatin > transplatin > I > II > III > IV > V > L¹ > L² > L³ > L⁴ > L⁵ (Figure 5) and data are represented in supplementary material 6.

4.8 | DNA interaction studies

4.8.1 | Electronic absorption titration spectroscopy

Electronic absorption titration spectroscopy is most useful spectroscopic method for examine the interaction of substituted pyrazolo[1,5-a]pyrimidine based ligands (L¹-L⁵) and cyclometalated heteroleptic platinum(II)

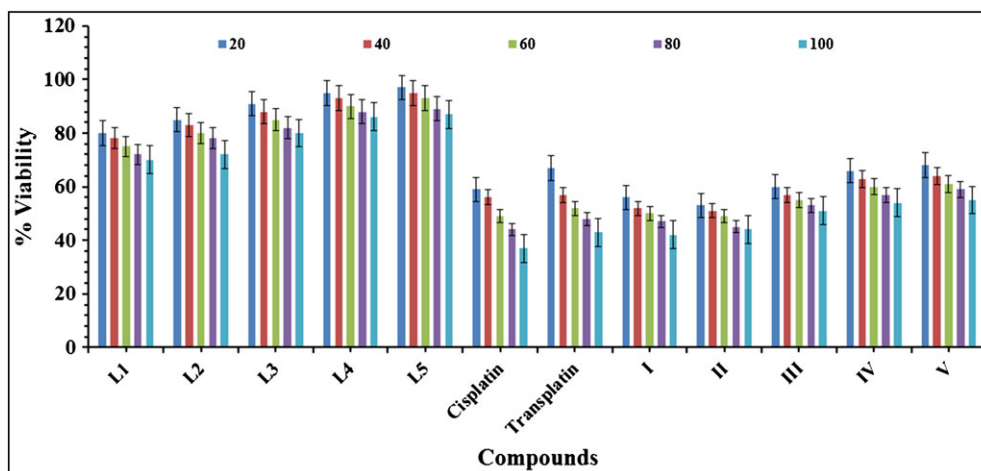


FIGURE 5 Percentage viability of the synthesized ligands (L¹-L⁵), cisplatin, transplatin and cyclometalated platinum(II) complexes (I-V) on *S. pombe* cells existing with standard deviation for three independent experiments

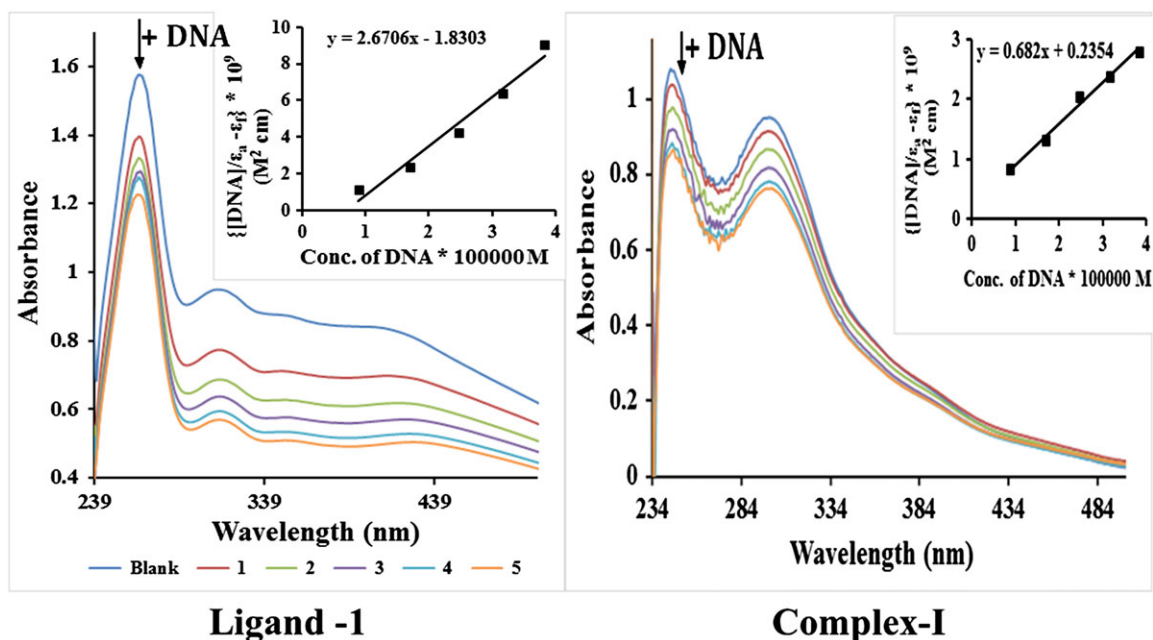


FIGURE 6 Electronic absorption spectra of ligand (L¹) and complex (I) in phosphate buffer pH = 7.2 at 25 °C in presence of increasing amount of HS-DNA

complexes with HS-DNA. A compounds interaction with HS-DNA through intercalative mode of binding is a result of hypochromism and bathochromism.^[38] The electronic absorption titration spectra of the ligand (L^1) and cyclometalated platinum(II) complex (I) in the absence and presence of HS-DNA are represented in Figure 6. The strong absorption bands of the synthesized ligands (L^1 - L^5) and complexes (I-V) are found in between

TABLE 1 The binding constant (K_b , M^{-1}), % hypochromicity and change in Gibb's free energy (ΔG^0 , $Jmol^{-1}$) of organometallic platinum(II) complexes (I-V) and pyrazolo[1,5-a]pyrimidine derivatives ligands (L^1 - L^5) with DNA.

Compounds	λ_{max} (nm)	$^a\Delta\lambda$ (nm)	bK_b (M^{-1}) $\times 10^5$	$^cH\%$	$^d\Delta G^0$ ($Jmol^{-1}$)
L^1	267 265	2	1.459	20.01	-29,460.00
L^2	269 267	2	0.858	34.50	-28,144.65
L^3	275 272	3	0.532	27.98	-26,960.47
L^4	308 302	5	0.286	29.29	-25,422.76
L^5	268 267	1	0.242	33.86	-25,008.87
I	243 238	1	2.890	37.14	-31,153.44
II	269 267	1	2.820	17.67	-31,092.69
III	272 267	2	2.776	18.55	-31,053.73
IV	273 271	2	2.325	30.32	-30,614.47
V	247 244	3	2.243	19.59	-30,525.51

^a $\Delta\lambda$ = Difference between bound wavelength and free wavelength.

^b K_b = Intrinsic DNA binding constant determined from the UV-visible absorption spectral titration.

^c $H\%$ = $[(A_{free} - A_{bound})/A_{free}] \times 100\%$.

^d ΔG^0 = Change in Gibb's free energy.

wavelength at about 234 to 308 nm.^[39] Therefore, the experimental obtained hypochromic effect in the intraligand transition band proposes that the compounds bind to HS-DNA via partial intercalative mode. The magnitude of binding strength of all the compounds with HS-DNA are considered through the value of binding constant (K_b), which is calculated by monitoring changes in the absorbance at the resultant λ_{max} with increasing concentrations of HS-DNA by the Wolfe-Shimer equation.^[40] The intrinsic binding constant K_b is determined the ratio of slope and intercept in plots of $[DNA]/(\epsilon_a - \epsilon_f)$ versus $[DNA]$ (Figure 6). The binding constant (K_b) values of synthesized pyrazolo[1,5-a]pyrimidine based ligands (L^1 - L^5) and cyclometalated platinum(II) complexes (I-V) are obtained in range of 0.242 - $1.459 \times 10^5 M^{-1}$ and 2.243 - $2.890 \times 10^5 M^{-1}$, respectively. It's concluded that the complexes have higher binding affinity as compared to ligands. Binding constant (K_b) of the ethidium bromide is $7.1 \times 10^5 M^{-1}$, it is higher than synthesized compounds. The K_b values of cisplatin, oxaliplatin and carboplatin are $5.73 \times 10^4 M^{-1}$ ^[41], $5.3 \times 10^3 M^{-1}$ ^[42] and $0.33 \times 10^3 M^{-1}$ ^[43], respectively and these K_b values are comparable to synthesized cyclometalated platinum(II) complexes and ligands. Moreover, the percentage hypochromism ($H\%$) of the synthesized ligands (L^1 - L^5) and complexes (I-V) are observed in between 20.01-34.50%. The Gibb's free energy of the synthesized compounds are found negative values in the range of -25.00 to $-31.15 kJmol^{-1}$ representing the spontaneity of compound-DNA binding. The results of the compound bind to DNA more spontaneously in order of $I > II > III > IV > V > L^1 > L^2 > L^3 > L^4 > L^5$. The DNA binding data of the synthesized compounds are represented in Table 1.

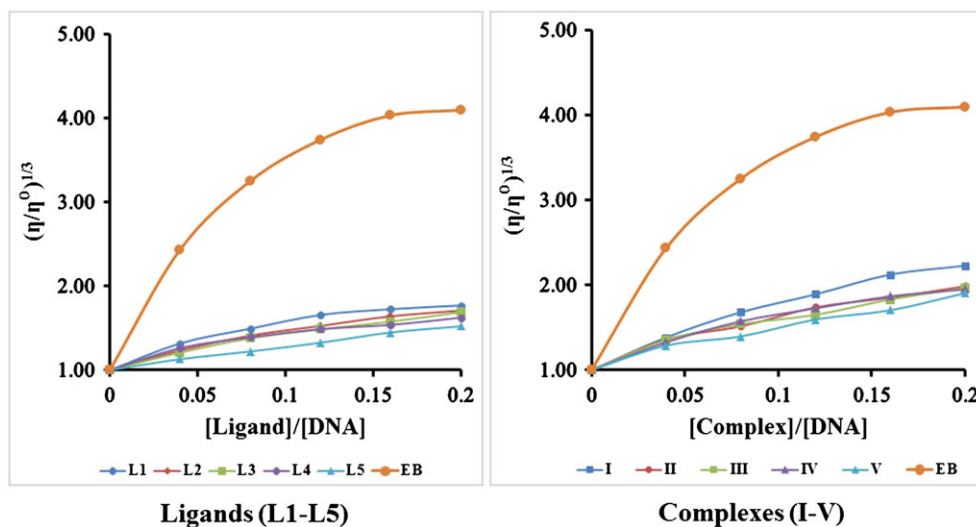


FIGURE 7 Effect of increasing amounts of ligands (L^1 - L^5) and complexes (I-V) on specific relative viscosity of HS-DNA. $1/R = [complex]/[DNA]$ ratio of 0.0, 0.04, 0.08, 0.12, 0.16, 0.20

4.8.2 | Viscosity measurements

The special effects of the synthesized ligands and complexes on the relative viscosity of HS-DNA has been represented in Figure 7. The viscosity of all the compounds is slightly increase with HS-DNA as comparable to EB, suggesting the partial intercalative mode of binding and this result is similar to the electronic absorption titration spectroscopic data. The observed relative viscosity of the synthesized ligands and complexes are in order of $EB > I > II > III > IV > V > L^1 > L^2 > L^3 > L^4 > L^5$.

4.8.3 | Interaction of the complexes with DNA by fluorescence spectroscopic method

In fluorescence quenching study, ethidium bromide (EtBr) as a cationic dye that is normally used for DNA interaction

TABLE 2 Linear stern-Volmer quenching constant (K_{sv}), binding sites (n) and association binding constant (K_a) calculated from double logarithmic plots for the interaction of complex with HS-DNA.

Complexes	K_{sv} (M^{-1})	K_a (M^{-1})	n	ΔG (J mol ⁻¹)
I	1.40×10^2	5.01×10^5	1.4212	-32,517.48
II	7.1×10^3	1.76×10^5	1.3505	-29,937.18
III	5.9×10^3	1.73×10^4	1.1148	-24,187.30
IV	2.6×10^3	5.05×10^3	1.1162	-21,127.23
V	6.8×10^3	0.93×10^3	0.8124	-16,961.00

via intercalation. Upon EB-DNA interaction, characteristic of EtBr shows the changes in absorbance, reflected by an enhancement in fluorescence intensity by about one order of magnitude, as compared to free dye in solution. Hence, when a platinum(II) complexes are added to the EB-DNA system, any quenching of the fluorescence will indicate the replacement of EB by the coordination molecule (DNA), via intercalative mode, it is expected of its strong stacking interaction between the adjacent DNA base pairs.

Fluorescence quenching analysis has been carried out for platinum(II) complexes and the corresponding emission spectra of the EB-DNA solutions in the presence of the increasing amounts of complex concentrations ($r = 0.33$ to 3.33), fluorescence quenching data of all complexes and graph are represented in supplementary material 7. Which clearly indicate a dramatic increase in the fluorescence intensity of the EB-DNA by adding the Pt(II) complex. In DNA-EB system, the increase of the fluorescence intensity is due to releasing free EB molecules. Therefore, the formation of complex-DNA stops the binding of EB and the complete metal complex-DNA formation occurs when the study fluorescence intensity is sufficient.^[25]

Moreover, the Stern-Volmer quenching constants (K_{sq}), change in standard Gibb's free energy (ΔG^0) and associative binding constant (K_a) of platinum(II) complexes are observed in range of 1.40×10^2 – $7.1 \times 10^3 M^{-1}$, -12.37 to $-32.51 kJmol^{-1}$ and 0.15×10^3 – $5.05 \times 10^3 M^{-1}$, respectively (Table 2). The corresponding plots obtained

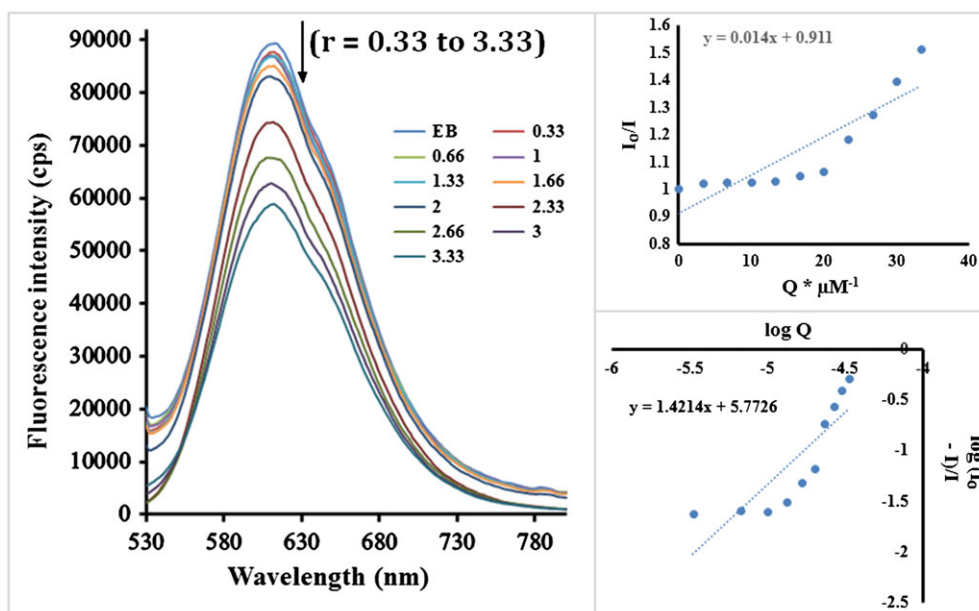


FIGURE 8 Fluorescence emission spectra of EB bound to HS-DNA in the presence of complexes (I). [EB] = $33.3 \mu M$, [DNA] = $10 \mu M$; [complex] = (i) 3.33, (ii) 6.66, (iii) 10, (iv) 13.33, (v) 16.66, (vi) 20, (vii) 23.33, (viii) 26.66, (ix) 30, (x) $33.3 \mu M$; λ_{ex} = 510 nm. The arrows show the intensity changes upon increasing the concentrations of complex. Inset graph: Plots of I_0/I vs. $[Q]$, with • for the experimental data points and the full line for the linear fitting of the data. Comparative plot of $\log[I_0/I]$ versus $\log[\text{complex}]$ for the titration of HS-DNA EB system with platinum(II) complexes (I) in phosphate buffer medium

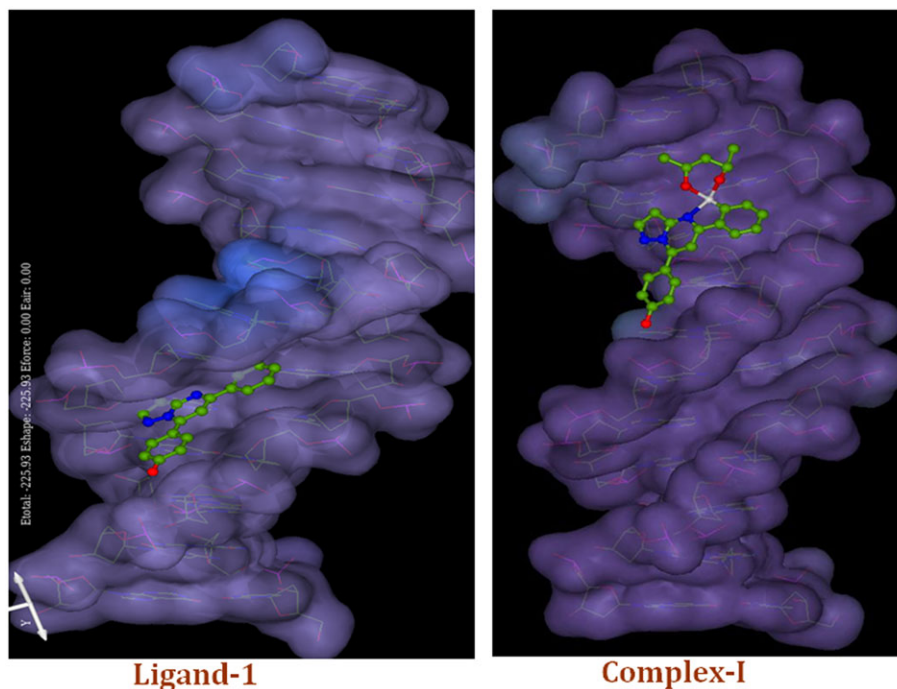


FIGURE 9 Molecular docking model of ligand (L^1) and complex (I) (ball and stick) with DNA helix (PDB ID: 1BNA) (VDW spheres) of sequence d(ACCGACGTCGGT)2. The compounds is docked with DNA base pairs via partial intercalation mode

from the experimental quenching data for the complexes are shown in Figure 8.

4.8.4 | Molecular modeling study

The synthesized compound can play an important role in the improvement of new chemotherapeutic drugs that lead to the recognition of specific sequences and structures of nucleoside and nucleotide.^[44] Molecular docking study displays a very significant role to understanding the mechanistic pathway of complex-DNA interactions, by placing the complex penetrate binding site of the DNA helix. The substituted pyrazolo[1,5-a]pyrimidine based ligands (L^1 - L^5) and cyclometalated heteroleptic platinum(II) complexes (I-V) are docked with in a DNA double helix structure by molecular docking analysis. Which is represented in Figure 9 and supplementary material 8. Thus, in order to check and illuminate the obtained spectroscopic results and to get a further insight into the intercalation ability, platinum(II) complexes (I-V) and ligands (L^1 - L^5) docked with DNA double helix structure. The complexes under investigation bind with B-DNA (PDB ID: 1BNA) at the A-T rich via partial intercalation mode.^[45] Furthermore, the DNA in such a way that the part of the planar heterocyclic ring containing ligands and complexes including outside edge stacking interaction with oxygen atoms of the phosphate backbone and further stabilized by Van der Waals interactions, hydrophobic contacts and

hydrogen bonding with the DNA functional groups that define the partial intercalation.^[46,47] The binding energies of the docked cyclometalated platinum(II) complexes (I-V) with DNA are -278.81 (I), -284.92 (II), -280.91 (III), -286.02 (IV) and -286.08 (V), respectively. The binding energies of the pyrazolo[1,5-a]pyrimidine based ligands (L^1 - L^5) with DNA are -225.93 (L^1), -227.33 (L^2), -228.00 (L^3), -233.25 (L^4) and -228.12 (L^5), respectively. The platinum(II) complexes exhibit higher binding affinity with DNA as compared to pyrazolo[1,5-a]pyrimidine

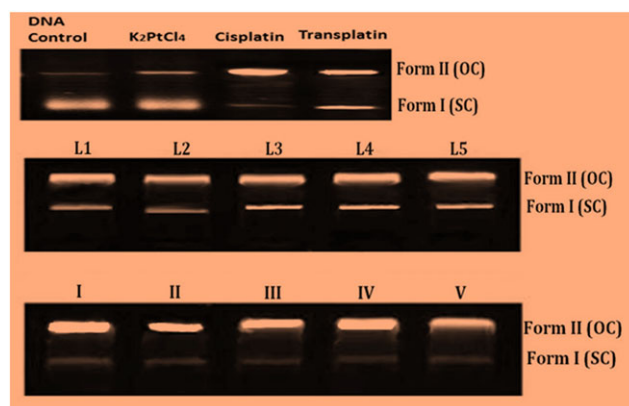


FIGURE 10 Photogenic view of cleavage of pUC19 DNA ($300 \mu\text{g}/\text{cm}^3$) with series of ligands (L^1 - L^5) and Pt(II) complexes ($200 \mu\text{M}$) using 1% agarose gel containing $0.5 \mu\text{g}/\text{cm}^3$ EtBr. Reactions were incubated in TE buffer solution (pH 8) at a final volume of 15 mm^3 for time period of 3 h at 37°C

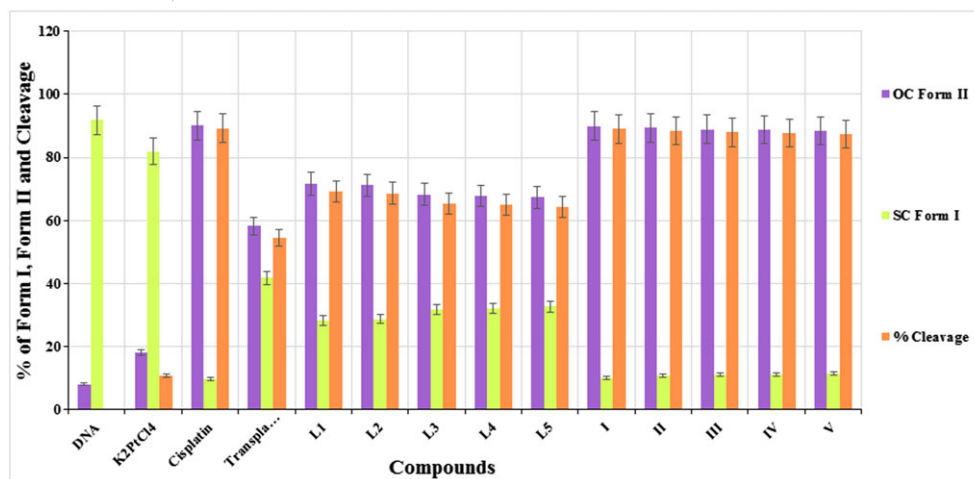


FIGURE 11 Plot of nuclease cleavage (% of form I, form II and DNA cleavage) assay of the ligands (L¹-L⁵) and complexes (I-V). Error bars represent standard deviation of three replicates ($\pm 5\%$)

based ligands. The compound interact with DNA, to provide greater binding affinity obtained by molecular docking study is in agreement with the experimental results developed from electronic absorption titration, viscosity measurements and fluorescence studies.

4.8.5 | Photochemical analysis of DNA nuclease activity

The effect of the compounds on DNA is estimated by their DNA-cleavage ability.^[48,49] Which can be determined by the cleavage mechanism. The cleavage efficiency of these molecules has usually examined by agarose gel electrophoresis.^[50,51] The cyclometalated platinum(II) complexes, cisplatin, transplatin and pyrazolo[1,5-a]pyrimidine based ligands are promote the percentage cleavage of pUC19 DNA from supercoiled Form I to the open circular Form II (Figure 10). The control experiment using DNA alone does not show any significant cleavage of DNA (Lane 1). A slight cleavage is observed when K₂PtCl₄ salt has been added to the DNA (Lane 2). A significant cleavage of the supercoiled form to open circular form is observed, when cisplatin, transplatin and platinum(II) complexes is added to the DNA (Lane 3-9). The % cleavage graph for all the compounds can be calculated using AlphaDigiDoc™ RT Version V.4.1.0 PC-Image software. And % cleavage data of the synthesized compounds are represented in supplementary material 9. The % cleavage ability of the all compounds is arrange in order of cisplatin > I > II > III > IV > V > L¹ > L² > L³ > L⁴ > L⁵ > transplatin > K₂PtCl₄. The complexes (I-V) and cisplatin exhibits greater DNA cleavage affinity as compared to ligands (L¹-L⁵), transplatin and K₂PtCl₄ salt at the same

concentration. The Figure 11 represent percentage cleavage of compounds.

5 | CONCLUSION

A series of cyclometalated platinum(II) complexes and pyrazolo[1,5-a]pyrimidine based ligands have been synthesized. The synthesized compounds have been characterized by the spectroscopic and physicochemical techniques such as ¹H NMR, ¹³C NMR, FT-IR, electronic spectral study, mass spectroscopy, magnetic moment, molar conductivity, TGA and elemental analysis. The platinum(II) complexes have square planar geometry and diamagnetic in nature. DNA binding activities of the synthesized compounds have been carried out using electronic absorption titration spectroscopy, fluorescence quenching analysis, viscosity measurements and molecular docking study. These studies suggest partial intercalation mode of binding. The complexes exhibit highest binding ability and binding strength as compared to ligands. The binding constant (K_b) of complex (I) is higher than other compound because of the complex (I) containing highly electron withdrawing functional group (-F atom). The complexes and cisplatin exhibit effective DNA cleavage as compared to ligands, transplatin and K₂PtCl₄ salt. The platinum(II) complexes and cisplatin exhibit excellent *in vitro* brine shrimp cytotoxicity activity as compared to ligands and transplatin. *In vitro* cellular level cytotoxicity bioassay of the synthesized platinum(II) complexes, cisplatin, transplatin and ligands have been carried out using *S. Pombe* cells. The % viability of the platinum(II) complexes is comparable to the cisplatin and higher as compared to transplatin and ligands. The minimum inhibitory concentration of the synthesized

compounds have been carried out using five different bacterial species. The platinum(II) complexes (I-V) show higher potency against two Gram^(+ve) and three Gram^(-ve) microorganism. Further studies are necessary to evaluate precise molecular mechanism of cytotoxicity and the pharmacological properties to reveal the actual mechanism of the biological activity.

ACKNOWLEDGEMENTS

The authors are thankful to the Head, Department of Chemistry, Sardar Patel University, Vallabh Vidyanagar, Gujarat, India, for providing necessary research facilities, DST-PURSE, Sardar Patel University, Vallabh Vidyanagar for mass spectral analysis. The authors gratefully acknowledge the University Grants Commission, New Delhi, India for meritorious fellowships awarded to them during year 2014-2018 and "BSR UGC One Time Grant", vide UGC letter no. F.19-119/2014 (BSR).

DECLARATION OF INTEREST

The authors report no conflicts of interest. The authors alone are responsible for the content and writing of the paper.

ORCID

Mohan N. Patel  <http://orcid.org/0000-0001-9016-9245>

REFERENCES

- [1] H. Li, J. Ding, Z. Xie, Y. Cheng, L. Wang, *J. Organomet. Chem.* **2009**, *694*, 2777.
- [2] A. Guida, M. H. Lhouty, D. Tichit, F. Figueras, P. Geneste, *Appl. Catal., A* **1997**, *164*, 251.
- [3] V. V. Lipson, S. M. Desenko, V. V. Borodina, M. G. Shirobokova, *Chemistry of Heterocyclic Compounds* **2007**, *43*, 1544.
- [4] J. Sun, J.-K. Qiu, B. Jiang, W.-J. Hao, C. Guo, S.-J. Tu, *The Journal of Organic Chemistry* **2016**, *81*, 3321.
- [5] J. J. Mousseau, A. Fortier, A. B. Charette, *Org. Lett.* **2010**, *12*, 516.
- [6] A. Liang, Y. Li, W. Zhu, Y. Wang, F. Huang, H. Wu, Y. Cao, *Dyes Pigm.* **2013**, *96*, 732.
- [7] C.-L. Ho, W.-Y. Wong, B. Yao, Z. Xie, L. Wang, Z. Lin, *J. Organomet. Chem.* **2009**, *694*, 2735.
- [8] M. Patra, M. Wenzel, P. Prochnow, V. Pierroz, G. Gasser, J. E. Bandow, N. Metzler-Nolte, *Chem. Sci.* **2015**, *6*, 214.
- [9] B. N. M. N. R. Ferrigni, *Journal of Medicinal Plant Research* **1982**, *45*, 31.
- [10] S. M. R. I. M. R. Islam, A. S. M. Noman, J. A. Khanam, S. M. M. Ali, M. W. Lee, *Mycobiology* **2007**, *35*, 25.
- [11] S. C. Karad, V. B. Purohit, D. K. Raval, *Eur. J. Med. Chem.* **2014**, *84*, 51.
- [12] M. E. Reichmann, S. A. Rice, C. A. Thomas, P. Doty, *J. Am. Chem. Soc.* **1954**, *76*, 3047.
- [13] J. Marmur, *J. Mol. Biol.* **1961**, *3*, 208.
- [14] T. M. H. Paul, M. G. B. Drew, P. Chattopadhyaya, *J. Coord. Chem.* **2012**, *65*, 1289.
- [15] Z.-Y. Y. Yong Li, M.-F. Wang, *J. Fluoresc.* **2010**, 891.
- [16] S. Ramakrishnan, E. Suresh, A. Riyasdeen, M. A. Akbarsha, M. Palaniandavar, *Dalton Transactions* **2011**, *40*, 3524.
- [17] J. B. Chaires, N. Dattagupta, D. M. Crothers, *Biochemistry* **1982**, *21*, 3933.
- [18] F. Leng, W. Priebe, J. B. Chaires, *Biochemistry* **1998**, *37*, 1743.
- [19] J. R. Lakowicz, **2006**.
- [20] L. Zhu, K. Zheng, Y.-T. Li, Z.-Y. Wu, C.-W. Yan, *J. Photochem. Photobiol., B* **2016**, *155*, 86.
- [21] O. Stern, M. Volmer, *Z. Phys.* **1919**, *20*, 183.
- [22] R. Frank, H. Rau, *The Journal of Physical Chemistry* **1983**, *87*, 5181.
- [23] A. Kathiravan, R. Renganathan, *Polyhedron* **2009**, *28*, 1374.
- [24] K. P. Thakor, M. V. Lunagariya, M. N. Patel, *J. Biomol. Struct. Dyn.* **2016**, *1*.
- [25] M. Hong, G. Chang, R. Li, M. Niu, *New J. Chem.* **2016**, *40*, 7889.
- [26] C. G. Ricci, P. A. Netz, *J. Chem. Inf. Model.* **2009**, *49*, 1925.
- [27] J. V. Mehta, S. B. Gajera, M. N. Patel, *J. Biomol. Struct. Dyn.* **2016**, *1*.
- [28] D. Sinha, A. K. Tiwari, S. Singh, G. Shukla, P. Mishra, H. Chandra, A. K. Mishra, *Eur. J. Med. Chem.* **2008**, *43*, 160.
- [29] P. R. Reddy, A. Shilpa, *Polyhedron* **2011**, *30*, 565.
- [30] C. Shiju, D. Arish, N. Bhuvanesh, S. Kumaresan, *Spectrochim. Acta, Part A* **2015**, *145*, 213.
- [31] V. X. Jin, J. D. Ranford, *Inorg. Chim. Acta* **2000**, *304*, 38.
- [32] A. A. Soliman, O. I. Alajrawy, F. A. Ataby, W. Linert, *J. Mol. Struct.* **2016**, *1115*, 17.
- [33] R. Prabhakaran, A. Geetha, M. Thilagavathi, R. Karvembu, V. Krishnan, H. Bertagnolli, K. Natarajan, *J. Inorg. Biochem.* **2004**, *98*, 2131.
- [34] B. G. Tweedy, *Phytopathology* **1964**, *55*, 910.
- [35] P. Kalaivani, R. Prabhakaran, F. Dallemer, P. Poornima, E. Vaishnavi, E. Ramachandran, V. V. Padma, R. Renganathan, K. Natarajan, *Metallomics* **2012**, *4*, 101.
- [36] N. R. F. B. N. Meyer, J. E. Putnam, L. B. Jacobsen, D. E. Nichols, J. L. McLaughlin, *Planta Med.* **1982**, *45*, 31.
- [37] E.-J. Gao, F. Hong, M.-C. Zhu, C. Ma, S.-K. Liang, J. Zhang, L.-F. Li, L. Wang, Y.-Y. Li, J. Wei, *Eur. J. Med. Chem.* **2014**, *82*, 172.
- [38] C. Janiak, *J. Chem. Soc., Dalton Trans.* **2000**, 3885.
- [39] C. Protogeraki, E. G. Andreadou, F. Perdih, I. Turel, A. A. Pantazaki, G. Psomas, *Eur. J. Med. Chem.* **2014**, *86*, 189.
- [40] J. Liu, W. Zheng, S. Shi, C. Tan, J. Chen, K. Zheng, L. Ji, *J. Inorg. Biochem.* **2008**, *102*, 193.
- [41] C. N. N'Soukpoé-Kossi, C. Descôteaux, É. Asselin, H.-A. Tajmir-Riahi, G. Bérubé, *DNA Cell Biol.* **2007**, *27*, 101.
- [42] H. Soori, A. Rabbani-Chadegani, J. Davoodi, *Eur. J. Med. Chem.* **2015**, *89*, 844.
- [43] A. Paul, S. Anbu, G. Sharma, M. L. Kuznetsov, B. Koch, M. F. C. Guedes da Silva, A. J. L. Pombeiro, *Dalton Transactions* **2015**, *44* 19983.
- [44] D. R. Boer, A. Canals, M. Coll, *Dalton Transactions* **2009**, 399.
- [45] V. Thamilarasan, P. Karunakaran, N. Kavitha, C. Selvaraju, N. Sengottuvelan, *Polyhedron* **2016**, *118*, 12.
- [46] M. Baginski, F. Fogolari, J. M. Briggs, *J. Mol. Biol.* **1997**, *274*, 253.

- [47] J.-G. Liu, Q.-L. Zhang, X.-F. Shi, L.-N. Ji, *Inorg. Chem.* **2001**, *40*, 5045.
- [48] A. M. Pyle, J. P. Rehmann, R. Meshoyrer, C. V. Kumar, N. J. Turro, J. K. Barton, *J. Am. Chem. Soc.* **1989**, *111*, 3051.
- [49] J. Qian, W. Gu, H. Liu, F. Gao, L. Feng, S. Yan, D. Liao, P. Cheng, *Dalton Transactions* **2007**, 1060.
- [50] B. Macías, M. V. Villa, B. Gómez, J. Borrás, G. Alzuet, M. González-Álvarez, A. Castiñeiras, *J. Inorg. Biochem.* **2007**, *101*, 444.
- [51] A. K. Sadana, Y. Mirza, K. R. Aneja, O. Prakash, *Eur. J. Med. Chem.* **2003**, *38*, 533.

SUPPORTING INFORMATION

Additional Supporting Information may be found online in the supporting information tab for this article.

How to cite this article: Lunagariya MV, Thakor KP, Patel NJ, Patel MN. Synthesis, characterization and biological application of cyclometalated heteroleptic platinum(II) complexes. *Appl Organometal Chem.* 2017;e4045. <https://doi.org/10.1002/aoc.4045>